Atmospheric Research 305 (2024) 107423

Contents lists available at ScienceDirect

Atmospheric Research

journal homepage: www.elsevier.com/locate/atmosres

Characterization of cross-continental $PM_{2.5}$: Insights into emissions and chemical composition

Caroline Scaramboni [a,b,*,1], Camila Novais Farias [c,a,1], Pérola de Castro Vasconcellos [c], Michael Levi [a], Ioannis Sadiktsis [d], Simone Andréa Pozza [e], Gisela de Aragão Umbuzeiro [e], Tetsushi Watanabe [f], Poliany Cristiny de Oliveira Rodrigues [g], Adriana Grandis [h], Débora Pagliuso [h], Marcos Silveira Buckeridge [h], Maria Lucia Arruda Moura Campos [b], Maria Kippler [a], Kristian Dreij [a], Marcos Felipe de Oliveira Galvão [a,*]

[a] Institute of Environmental Medicine, Karolinska Institutet, Box 210, Stockholm SE-171 77, Sweden
[b] Department of Chemistry, Faculty of Philosophy, Science and Letters at Ribeirão Preto, University of São Paulo, Ribeirão Preto 14040-901, SP, Brazil
[c] Chemistry Institute, University of São Paulo, São Paulo, Brazil
[d] Department of Materials and Environmental Chemistry, Stockholm University, Stockholm SE-106 91, Sweden
[e] Faculdade de Tecnologia, Universidade Estadual de Campinas (UNICAMP), Limeira, Brazil
[f] Department of Public Health, Kyoto Pharmaceutical University, Kyoto, Japan
[g] Faculty of Health Sciences, Mato Grosso State University (UNEMAT), Cáceres, Brazil
[h] Department of Botany, Institute of Biosciences, University of São Paulo, São Paulo, Brazil

ARTICLE INFO

Keywords:
Particulate matter
Polycyclic aromatic hydrocarbons
Monosaccharide anhydrides
Inorganic elements
Biomass burning markers

ABSTRACT

Atmospheric fine particulate matter ($PM_{2.5}$) is a critical indicator of air quality, with substantial implications for human health. Understanding the emission sources and chemical composition of $PM_{2.5}$ is crucial for mitigating possible adverse health effects. This study spans five diverse cities on three continents from north and south hemisphere: Stockholm (Sweden), Kyoto (Japan), Limeira, Ribeirão Preto, and Cáceres (Brazil). Our objective was to assess $PM_{2.5}$ chemical composition and regional and long-range transport influences to identify the main sources of particulate air pollution at these cities during the winter/dry seasons. All studied cities but Kyoto exhibited $PM_{2.5}$ levels above World Health Organization (WHO) guidelines, with the Brazilian cities experiencing the highest fine particle pollution levels, implying increased adverse health risks. We observed significant variations in concentrations of polycyclic aromatic compounds (PACs), monosaccharide anhydrides (MAs), and inorganic elements. Limeira exhibited the highest levels of total PACs (median level of 12.4 ng m^{-3}), while Cáceres displayed high variability of PACs, most likely due to episodic regional wildfire events. MA concentrations were significantly higher in Limeira and Ribeirão Preto and together with elevated levels of retene and potassium (K) they suggested a substantial influence of biomass burning. Backward air mass trajectory analysis suggested widespread Amazon and Savanna wildfires along with local fires as main contributors for these sites. All source identification approaches highlighted differences among the cities, with Stockholm and Kyoto showing influence of sources related to traffic emissions, waste burning, and long-range transport, and Brazilian cities traffic, industrial, biogenic, and more evident biomass burning. This cross-continental study provides valuable insights into $PM_{2.5}$ composition and emission sources, emphasizing the impact of different emissions on air quality. Our findings underscore the importance of local strategies to mitigate air pollution and protect public health, especially in regions where $PM_{2.5}$ levels consistently exceed recommended guidelines.

* Corresponding authors.
E-mail addresses: carolinesc@usp.br (C. Scaramboni), felipe.de.oliveira.galvao@ki.se (M.F. de Oliveira Galvão).
[1] These authors share first authorship

https://doi.org/10.1016/j.atmosres.2024.107423
Received 3 November 2023; Received in revised form 15 March 2024; Accepted 13 April 2024
Available online 18 April 2024

1. Introduction

Atmospheric particulate matter (PM) is a crucial indicator of air quality, as highlighted by the World Health Organization (WHO). Human exposure to PM is linked to adverse health effects, particularly respiratory and cardiovascular diseases and cancer (Hvidtfeldt et al., 2021; Wolf et al., 2021). The intricate PM composition in both urban and non-urban settings poses challenges in assessing its potential health risks, given its variations in size, chemical composition, and origins (WHO, 2021). However, air quality research has mainly focused on assessing levels and impact of pollutants in densely populated cities, while less is known about their associations in small-sized cities or non-urban sites (Liang and Gong, 2020). The determinants of PM levels and trends are not the same for cities at different developmental stage or geographic regions (Liang and Gong, 2020), and outdoor air pollution can be as severe in non-urban regions as in urban, with implications for monitoring, regulations, health, and policy (Ravishankara et al., 2020). Among PM size fractions, $PM_{2.5}$ holds significance due to its extended atmospheric residence time and ability to penetrate deep into the respiratory system (Schraufnagel et al., 2019). Consequently, the scientific community and policymakers have shown an increased interest in knowing the sources of $PM_{2.5}$ to develop cost-effective mitigation strategies. To guide such strategies, and to protect human health, the WHO recently presented updated recommended air quality guideline (AQG) levels for $PM_{2.5}$ (WHO, 2021).

The chemical composition of PM can vary significantly across seasons and geographical regions and depends on the emission sources, meteorological conditions, and atmospheric processing. Carbonaceous species, such as organic and elemental carbon, constitute a substantial fraction of urban $PM_{2.5}$ (Kelly and Fussell, 2012). Emissions of specific monosaccharides anhydrides (MAs) - levoglucosan, mannosan, and galactosan - are mainly associated with biomass burning since they are formed during the pyrolysis of cellulose and hemicellulose at temperatures >300 °C (Simoneit, 2002). These compounds are emitted in characteristic amounts and present different concentration ratios according to the type of biomass fuel burned (Suciu et al., 2019). Another class of organic compounds in PM are polycyclic aromatic compounds (PACs), some of which have known mutagenic and carcinogenic potentials (Mallah et al., 2022). They are formed during incomplete combustion of organic material, with sources including biomass burning, automobile exhaust, industrial power generation, incinerators, and production of coal tar, coke, and asphalt (Boström et al., 2002). The PACs include non-substituted polycyclic aromatic hydrocarbons (PAHs), emitted directly to the atmosphere, and their derivatives, such as nitrated, and oxygenated PAHs (OPAHs), which can be released directly and/or formed by photochemical reactions in the atmosphere (Idowu et al., 2019). Of the numerous PACs, only the PAH benzo[*a*]pyrene (BaP) has been assigned an annual reference level by the WHO (0.12 ng m^{-3}) and an annual target value by the EU (1 ng m^{-3}) for its cancer risk (WHO, 2000; EU 2004/107/EC).

Additionally, inorganic elements such as metals (e.g., Cd, Pb), metalloids (e.g., Si, As), and non-metals (e.g., S, Se) constitute an important portion of PM. For instance, atmospheric PM can be enriched with e.g., Si, Al, K, Ca from soil dust resuspension, or with specific metals such as Cr, Cd, and Pb from industrial activities and non-exhaust emissions from traffic (by mechanical abrasion of brakes and tire/road surface wear) (Calvo et al., 2013; Jandacka et al., 2022). Some metals and metalloids in PM also pose risks to human health since they can cause respiratory problems, cardiovascular disease, renal damage, neurological disorders, and various types of cancer (Vithanage et al., 2022). There are also WHO AQGs for chemicals of health concern, including Pb, As, Cd, and Ni (WHO, 2000).

This work presents a comprehensive characterization of $PM_{2.5}$ across five cities on three different continents, each characterized by unique meteorological conditions and emission sources, encompassing urban and non-urban characteristics. The cities were Stockholm (Sweden), Kyoto (Japan), Limeira, Ribeirão Preto, and Cáceres (Brazil). We have previously shown markedly different PAC concentrations in total suspended particles (TSP) collected at Stockholm, Kyoto, and Limeira, implying that the residents of these urban environments are exposed to different levels of genotoxic pollutants (Maselli et al., 2020). Our present study extended this research by conducting new $PM_{2.5}$ samplings in these three cities and in two additional Brazilian cities: Ribeirão Preto, a midsized agro-industrial city, and Cáceres, a town surrounded by state parks and an ecological reserve. The objective of the study was to identify the main sources of $PM_{2.5}$ in the five selected cities by performing a more comprehensive chemical characterization (i.e., 16 PAHs, 4 OPAHs, 3 MAs, and 15 inorganic elements) together with an analysis of air mass trajectories. This approach aimed at enhancing our knowledge of the diverse factors governing urban and non-urban air quality.

2. Materials and methods

2.1. Chemicals and solvents

The solvents acetonitrile and dichloromethane were HPLC-grade from Merck (USA). 2-propanol and acetone used to clean filter media were HPLC-grade from Rathburn Chemicals Ltd. (Walkerburn, Scotland, UK). Information about PACs, MAs, and element standards used in this work is listed in Table S1 in the supplementary material.

2.2. Air sampling

$PM_{2.5}$ sampling campaigns were carried out in 2020, 2021, and 2022 at five locations: Stockholm, Sweden (59°14′50.3"N; 17°50′35.1"E); Kyoto, Japan (34°59′18.0"N 135°48′42.0"E); Limeira (22°33′43.8"S; 47°25′20.8"W), Ribeirão Preto (21°09′40.7"S; 47°51′29.8"W) and Cáceres (15°26′45.5"S; 57°09′13.0"W), located in Brazil (Fig. 1).

The sampling site at Stockholm was situated next to a highway (European route E4/E20) with around 100,000 vehicles passing each day (Elmgren and Burman, 2020). In Kyoto, samples were collected at the Kyoto Pharmaceutical University in a residential area of Yamashina-ku (132,065 inhabitants in 2022; Yamashina Website, 2023). Regarding the cities in Brazil, Limeira and Ribeirão Preto are both located in the São Paulo State, the most populous state in the country (IBGE, 2022). The sampling site in Limeira (291,869 inhabitants and 138,918 vehicles in 2022) was located at the School of Technology of the University of Campinas at ~2 km from the city center. In Ribeirão Preto (698,259 inhabitants and 308,643 vehicles in 2022), samples were collected at the University of São Paulo campus, located at the suburban area of the city, ~1 km distant from extensive sugarcane plantations. In turn, Cáceres (89,478 inhabitants and 18,049 vehicles in 2022) is located in the Mato Grosso State, at the intersection of three different biomes: Amazon, Pantanal, and the Brazilian savanna (Cerrado), on the edge of an area known as the "deforestation arc". The sampling in Cáceres was carried out at a rural site located at a remote area. Satellite images illustrating the characteristics of sampling sites are available in the Supplementary Material (Fig. S1).

$PM_{2.5}$ samples were collected with the same batch of filters and similar samplers during the winter/dry season for all five cities. Borosilicate glass filters coated with fluorocarbon (Fiberfilm Filters, Pallflex® Filters, USA) were washed with 2-propanol and acetone under suction, dried at 100 °C for 1 h, and put in a desiccator (> 48 h) at room temperature before weighing. Samples were collected using high-volume air samplers with a $PM_{2.5}$ inlet at airflow rate of approximately 1 m^3 min^{-1} during 1–7 days, depending on the expected PM mass (Table 1). Flow rate accuracy was better than 5% according to the manufacturers' manuals. Field blanks were prepared using a filter treated in the same way as the samples, except that no air was drawn through the filter. $PM_{2.5}$ mass was determined by weighing the filters before and after sampling after being equilibrated in a desiccator for > 48 h at room temperature. Samples were stored in a freezer at −20 °C

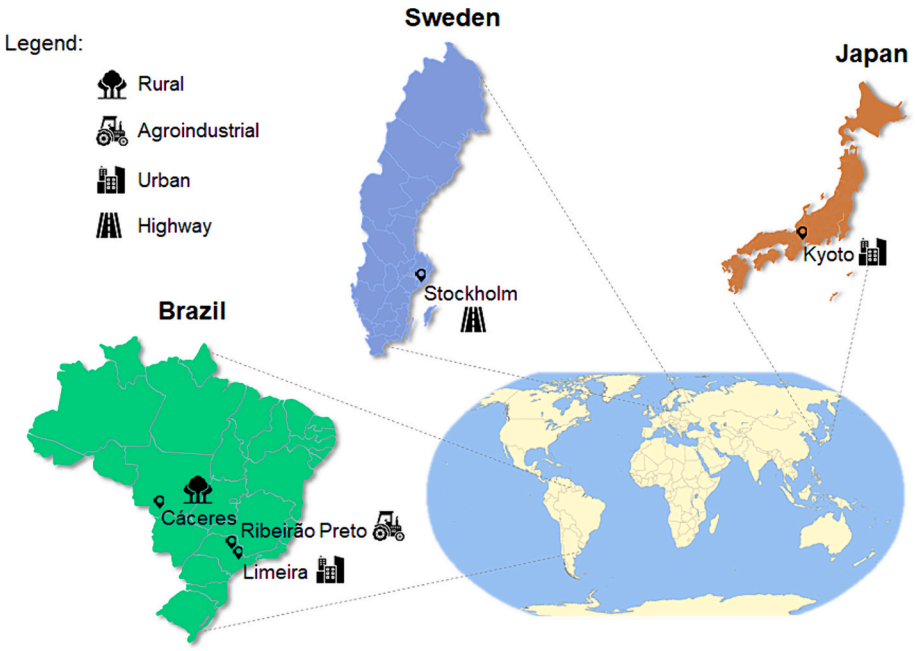

Fig. 1. Distribution of the five $PM_{2.5}$ sampling sites in different continents and countries. The map is not according to scale and for illustrative purposes only, created by combining open-source maps.

Table 1
Information about the sampling locations including $PM_{2.5}$ sampler, sampling period and season, number of filters, total sampling duration and air volume sampled.

Site	Sampler	Sampling period	Season	Total sampling duration (h)	Total air volume sampled (m^3)
Stockholm, Sweden	Acoem HiVol 3000 (Acoem, Melbourne, Australia)	February to March 2021 ($n = 5$)	Winter	538	35,629
Kyoto, Japan	Shibata Scientific Technology Model HV1000R $PM_{2.5}$ impactor (Soka, Japan)	February to March 2020 ($n = 9$)	Winter	1510	90,629
Limeira, Brazil	Tisch Environmental Model TE-6001 2.5I # Serie1362 (Cleves OH, USA)	September to October 2020 ($n = 9$)	Winter/ Spring	216	11,593
Ribeirão Preto, Brazil	Tisch Environmental Model TE-6001 2.5I # Serie1362 (Cleves OH, USA)	August to September 2021 ($n = 6$)	Winter	198	11,623
Cáceres, Brazil	Tisch Environmental Model TE-6001 2.5I # Serie1362 (Cleves OH, USA)	August 2022 ($n = 6$)	Winter	216	12,986

before extraction.

2.3. Determination of polycyclic aromatic compounds

PAHs and OPAHs were extracted and determined following the methodology described by Santos et al. (2016). Briefly, an area of 3.5 cm^2 of the samples and blank filters were extracted using micro-extraction devices (Whatmann MiniTM UniPrep Filters, Whatmann, USA) with 500 μL of acetonitrile:dichloromethane mixture (18:82%) for 23 min in an ultrasonic bath. The extracts were filtered and dried under a gentle stream of nitrogen gas. After resuspension and homogenization in 100 μL of the same solvent mixture, a volume of 1 μL was injected (splitless mode) in a gas chromatograph coupled to a mass spectrometer (GC/MS; Agilent GC 7820 A, MS 5975). The separation column was a DB-5 ms column (30 m × 0.250 mm, film thickness 0.25 μm) (Agilent Technologies, Folsom, CA, USA). The mass spectrometer was operated in electron impact mode (EI, 70 eV). Detection was performed using MS in selected ion monitoring (SIM) mode, in which two different ions were selected for each PAH and OPAH (Table S2).

The PAHs determined included low-molecular-weight (LMW-PAHs, 3-ring PAHs): phenanthrene (Phe) and anthracene (Ant); medium-molecular-weight (MMW, 4-ring PAHs): fluoranthene (Flt), pyrene (Pyr), retene (Ret), benz[*a*]anthracene (BaA), chrysene (Chr); and high-molecular-weight PAHs (HMW-PAHs, >5-ring PAHs): benzo[*b*]fluoranthene (BbF), benzo[*k*]fluoranthene (BkF), benzo[*e*]pyrene (BeP), benzo[*a*]pyrene (BaP), perylene (Per), indeno[1,2,3-*cd*]pyrene (InP), dibenz[*a*,*h*]anthracene (DBA), benzo[*ghi*]perylene (BPer) and coronene (Cor). The OPAHs determined were: 9-fluorenone (9-FLO), 9,10-anthraquinone (9,10-AQ), 2-methylanthraquinone (2-MAQ), and 7,12-benz[*a*]anthracenequinone (7,12-BaAQ).

The limits of detection (LOD) were defined by a signal-to-noise ratio of 3, while the limits of quantification (LOQ) were set as a signal-to-noise ratio of 10. The quantification was performed by external calibration, which presented good linearity ($r > 0.99$) (Table S3). The method's accuracy was evaluated with recovery tests and daily monitoring of standard solutions of the analytes studied (with an acceptable variation of up to 10%). Recovery tests were performed by spiking known amounts of standards to a filter, followed by extraction and analysis (Table S3). Final concentrations in the samples (Table S4) were subtracted by the determined amounts in the field blanks for each

corresponding sampling site.

2.4. Determination of monosaccharide anhydrides

Levoglucosan, galactosan, and mannosan were extracted from 3.5 cm^2 sections of the filters, following the methodology described by Gonçalves et al. (2021). Briefly, the filters were extracted with 10 mL of ultrapure water (Milli-Q, Millipore) for 30 min in an ultrasonic bath. After lyophilization, the dried extracts were resuspended in 500 μL of ultrapure water and filtered (0.22 μm, PTFE, Merck Millipore). The MAs were determined using a high-performance anion-exchange chromatography with pulsed amperometric detection equipped with a CarboPac SA10 column (ICS 5000 system, Dionex-Thermo). The analysis was performed by isocratic elution with 99.2% of water and 0.8% (*v*/v) sodium hydroxide (1 mL min^{-1}) (Pagliuso et al., 2018). The detection was made using a post-column base containing 500 mmol L^{-1} NaOH (0.5 mL min^{-1}) followed by a pulsed amperometric detector.

The LODs were defined by a signal-to-noise ratio of 3, while the LOQs were set as the lowest concentration of the calibration curves. The quantification was performed by external calibration, which presented good linearity ($r > 0.99$) (Table S3). Recovery tests were performed by spiking known amounts of standards to the filter, followed by extraction and analysis (Table S3). Final concentrations in the samples (Table S4) were subtracted by the determined amounts in the field blanks for each corresponding sampling site.

2.5. Determination of inorganic elements

Sample digestion and analysis were performed according to Kippler et al. (2021) with minor modifications described below. Sections of 3.5 cm^2 of the filters were digested in teflon tubes with 2 mL of concentrated nitric acid (67% *w*/w, Normatom Trace Analysis Grade, VWR, USA) and 3 mL of deionized water for 30 min (250 °C and at a pressure of 160 bar) in a Milestone ultraCLAVE II microwave digestion system (EMLS, Leutkirch, Germany). The digested solutions were allowed to cool to a temperature below 30 °C, after which they were diluted with deionized water to an acid concentration of 20%. Inductively coupled plasma mass spectrometer (Agilent 7900, Agilent Technologies, Tokyo, Japan), equipped with an octopole reaction system collision/reaction cell technology (with He or H_2 gas) to minimize spectral interferences was employed to determine elemental concentrations of the samples. The LODs and LOQs were calculated as three and ten times the standard deviation of the reagent blanks, respectively. The quantification was performed by external calibration, which presented good linearity ($r > 0.99$) (Table S3). Quality control was performed by including the digested reference materials Seronorm whole blood, batches 1,702,821 and 1,702,825 (SERO AS, Norway), and differences between obtained and recommended values are presented in Table S3. Final concentrations in the samples (Table S4) were subtracted by the determined amounts in the field blanks for each corresponding sampling site.

2.6. Analysis of enrichment factors

Enrichment factors (EF) were used to determine whether an inorganic element was found in greater abundance than expected from soil (natural) sources. The EFs were calculated according to Reimann and Caritat (2005). In this work, we used Fe as a reference element, and the concentrations of elements in the upper continental crust were taken from local references for Sweden (SGU, 2007), Japan (Yamasaki et al., 2013), and Brazil (de Coringa et al., 2014; Fadigas et al., 2006; Nogueira et al., 2018).

2.7. Backward air mass trajectories

To better understand the transport dynamics of $PM_{2.5}$, the origin of the air masses was performed using HYSLPIT 4.0 (HYbrid Single-Particle Lagrangian Integrated Trajectory) provided by the Air Resources Laboratory of the National Oceanic and Atmospheric Administration (NOAA, 2023). The simulations were conducted for each filter sampled in Stockholm, Kyoto, Limeira, Ribeirão Preto, and Cáceres using the Global Forecast System Reanalysis (GFS 0.25^0, global) to obtain meteorological data. The ending analyses were defined by the stop time of sampling for each filter, at an altitude of 500 and 2000 m above ground level. Trajectories were calculated every 6 h and the total running time was set up to 48 h for all filters.

2.8. Statistical analysis

The normality of the data was evaluated using the Shapiro-Wilk test. Due to the non-normal distribution of the data, ranges and median values were reported. Correlations between measured concentrations of air pollutants were performed using Spearman's rank correlation with two-tailed *p*-values. The criterion for significance was set at $p < 0.05$. Principal component analysis (PCA, two axes) was applied to the main chemical markers (37 variables and 35 samples, pg m^{-3}) using GraphPad Prism 9 statistical software (GraphPad Inc.). Before statistical analysis, values below LOD (16%) were substituted by LOD/2, and all the values were log-transformed and unit variance-scaled (Hites, 2019; Varmuza and Filzmoser, 2009).

3. Results and discussion

3.1. Fine particulate matter ($PM_{2.5}$)

The study spanned from 2020 to 2022, encompassing the period of COVID-19 pandemic. Notably, the fluctuation in $PM_{2.5}$ concentrations and emission profiles during the pandemic versus pre- or post-pandemic phases presents a complex narrative, influenced by diverse factors such as regional lockdown measures and meteorological dynamics. In Stockholm, PM_{10}, $PM_{2.5}$, and NO_x concentrations decreased during the pandemic, primarily attributed to meteorological conditions, and reduced vehicular emissions (Sadiktsis et al., 2023). A study conducted in São Paulo State, Brazil revealed contrasting trends for agro-industrial regions, with PM_{10} levels increasing during the pandemic due to regional factors like large number of fires during the dry season of 2020 (Carvalho et al., 2023a).

The highest levels of $PM_{2.5}$ were found at Ribeirão Preto (15.7–62.7 μg m^{-3}; median 49.5 μg m^{-3}) and Limeira (13.8–54.9 μg m^{-3}; median 33.7 μg m^{-3}), while the lowest levels were obtained in Kyoto (6.1–12.8 μg m^{-3}; median 9.9 μg m^{-3}). Stockholm had nearly twice the $PM_{2.5}$ levels of Kyoto (9.5–25.4 μg m^{-3}; median 19.7 μg m^{-3}). Cáceres had the highest variability in $PM_{2.5}$ levels, which ranged from 2.2 to 122.3 μg m^{-3}, with a median of 13.9 μg m^{-3}.

To assess the air quality at these sites, and because the sampling was performed during a short period of time, we compared the determined concentrations with the WHO's short-term (24-h) AQG for $PM_{2.5}$ of 15 μg m^{-3} (WHO, 2021). While all samples from Kyoto were below this level, all samples from Ribeirão Preto were above, and the other cities had samples both below and above the AQG. Previous studies performed in these cities/countries have shown that PM levels are higher during the winter/dry season compared to the summer/wet season (de Oliveira Galvão et al., 2018; Sadiktsis et al., 2023). Because we collected samples during winter/dry season, the $PM_{2.5}$ data presented here are higher or similar to annual $PM_{2.5}$ means reported by the local environmental agencies: Stockholm in 2021 6.0 μg m^{-3} (SLB, 2021), Kyoto in 2020 11.3 μg m^{-3} (National Institute for Environmental Studies, 2023), Limeira in 2020 12.0 μg m^{-3} (CETESB, 2020), and Ribeirão Preto in 2021 21.0 μg m^{-3} (CETESB, 2021). All these annual means were above the annual AQG of 5 μg m^{-3} recommended by WHO.

We could not find any annual data from local monitoring stations in Cáceres, but modeled satellite estimates suggested an annual $PM_{2.5}$ of 15.3 μg m^{-3} in 2021 (data provided by de Oliveira et al., 2023). To our

knowledge, this is the first study to collect *in loco* and analyze $PM_{2.5}$ levels and chemical composition in Cáceres. Notably, the $PM_{2.5}$ concentrations ranged up to 122.3 μg m^{-3} in Cáceres during the sampling period, indicating the importance of continuous monitoring. Currently, few states in the Legal Brazilian Amazon region have an air quality monitoring network (de Oliveira et al., 2023), although low-cost sensors are a viable initiative in inaccessible areas (Bi et al., 2022; Bousiotis et al., 2023). Exceeding both 24-h and annual AQG suggests an increased risk of mortality, and efforts should be made to improve the air quality in areas affected (Liu et al., 2019).

3.2. Polycyclic aromatic compounds (PACs)

The concentrations of PACs found in $PM_{2.5}$ collected at the five cities are presented in Table 2. Limeira had the highest median of total PAHs (Σ_{16}PAH), followed by Ribeirão Preto, Stockholm, Kyoto, and Cáceres. Σ_{16}PAH median in Limeira was 5.7 times higher than in Stockholm and 7.0 times higher than in Kyoto, similar to what has been observed in previous work for TSP samples collected in the same three cities in 2013–2014 (Maselli et al., 2020). However, our prior research indicated higher PAH concentrations in Kyoto compared to Stockholm, while in this study, the opposite was observed. This discrepancy is likely attributable to the different sampling location in Stockholm, now positioned adjacent to a heavily trafficked highway, implying greater PAC inputs. While Cáceres had the lowest median, it displayed the highest variation of Σ_{16}PAH concentration, with a difference of ~2 orders of magnitude between the minimum and maximum. This corroborates with the high variability observed in $PM_{2.5}$ levels. Although low concentrations were expected at the rural Cáceres site due to its remote location, it is likely that occasional $PM_{2.5}$ inputs were the main drivers of the elevated concentrations detected in certain samples.

Among the PAHs, human exposure to high-molecular-weight PAHs (HMW-PAHs, $\geq$ 5 rings), such as BbF and BaP, are of special health concern due to their higher mutagenic and carcinogenic activity compared to smaller PAHs (Jarvis et al., 2014). Ribeirão Preto, Limeira, and Kyoto samples were dominated by HMW-PAHs (81%, 72%, and 68%, respectively). BbF and BPer were the most abundant HMW PAHs at all sites (10–20%), while levels of BaP ranged 5–10% of Σ_{16}PAH (Fig. 2). The predominance of these PAHs in Stockholm, Kyoto and Limeira was reported in previous studies and was associated with vehicular traffic (Maselli et al., 2020; Sadiktsis et al., 2023). The high abundance of these compounds was also observed by Carvalho et al. (2023b) in São Carlos (2015–2018), a city close to Limeira and Ribeirão Preto (~100 km) that presents similar economic characteristics. BaP is used as an indicator for assessing the health risk of airborne PAHs, and WHO has estimated an annual reference level of BaP at 0.12 ng m^{-3} corresponding to an excess lifetime cancer risk of one in 100,000 (WHO Europe, 2021). Based on this value, the EU set an air quality threshold for BaP at 1 ng m^{-3} to be achieved by the member states at the end of 2012 (WHO Europe, 2021). Although some individual samples exceeded the EU target level, all median concentrations of BaP (Table 2) were below the EU target level while only measurements in Stockholm and Kyoto were below the WHO reference level. This agrees with recent short and long-term monitoring studies in these cities (Lim et al., 2022; Maselli et al., 2020; Sadiktsis et al., 2023).

Cáceres displayed the highest concentrations of Ret, up to 1257 pg m^{-3} (10% of Σ_{16}PAH). Ret is formed from abietic acid during the incomplete combustion of softwood, so this compound is often used as a molecular tracer for biomass burning (Ramdahl, 1983), and was also the most abundant PAH in PM_{10} samples from other locations at the same state as Cáceres (de Oliveira Alves et al., 2014; de Oliveira Alves et al., 2011). For total OPAHs (Σ_4OPAH), a different behavior was observed compared to Σ_{16}PAH. While Limeira and Ribeirão Preto were again the cities with the highest concentrations, Cáceres had nearly twice the concentrations of Σ_4OPAH than Kyoto and Stockholm (Table 2). Among the OPAHs, 9,10-AQ was the most frequently detected, with the highest concentrations at all sites except Cáceres, where 2-MAQ was the predominant OPAH. 2-MAQ was also the most abundant OPAHs during the period of intense biomass burning (winter, August–October/2011) in a forest reserve site in the Amazon Basin (de Oliveira Galvão et al., 2018).

3.3. Monosaccharide anhydrides (MAs)

The concentrations of MAs (levoglucosan (L), mannosan (M) and galactosan (G)) found in $PM_{2.5}$ are shown in Table 3. The relative ratios between levoglucosan and the other two isomers (L/M and L/G) are also

Table 2
Concentration ranges and medians (pg m^{-3}) of polycyclic aromatic compounds (PACs), including polycyclic aromatic hydrocarbons (PAHs) and oxygenated PAHs (OPAHs), in the $PM_{2.5}$ samples collected in Stockholm, Kyoto, Limeira, Ribeirão Preto and Cáceres.

PAC (pg m^{-3})	Stockholm (n = 5)		Kyoto (n = 9)		Limeira (n = 9)		Ribeirão Preto (n = 6)		Cáceres (n = 6)	
	min–max	median	min–max	median	min–max	median	min–max	median	min–max	median
Phe	19–131	74	15–75	34	79–769	158	55–272	82	15–591	55
Ant	<LOD – 25	20	<LOD – 15	<LOD	15–173	40	<LOD – 97	18	<LOD – 109	17
Flt	70–395	187	43–340	180	167–2774	449	120–670	232	35–2042	114
Pyr	43–288	170	33–236	93	200–1794	444	111–544	271	25–1591	81
Ret	<LOD – 101	75	<LOD – 184	<LOD	15–334	131	<LOD – 488	62	27–1257	92
BaA	32–246	130	<LOD – 138	45	<LOD – 1330	236	<LOD – 958	169	20–913	99
Chr	42–190	147	26–185	65	<LOD – 1530	328	101–1219	235	<LOD – 459	57
BbF	84–457	212	57–604	310	<LOD – 5593	1122	113–5663	712	<LOD – 3335	140
BkF	29–181	124	26–241	144	55–2060	405	152–1956	324	<LOD – 1725	86
BeP	41–173	120	39–268	143	89–2623	874	302–2140	525	<LOD – 1934	66
BaP	<LOD – 144	114	<LOD – 186	90	57–1489	941	256–1885	475	<LOD – 1217	91
Per	<LOD – 48	33	<LOD – 58	<LOD	57–321	206	48–384	119	<LOD – 175	30
InP	23–143	82	<LOD – 280	94	<LOD – 1984	1009	74–2547	406	<LOD – 1982	73
DBA	<LOD – 46	<LOD	<LOD – 78	<LOD	<LOD – 362	155	<LOD – 653	<LOD	<LOD – 431	68
BPer	73–235	178	61–356	176	294–3163	1974	785–3497	1397	25–2734	160
Cor	36–137	85	<LOD – 630	74	39–2269	738	90–1543	457	<LOD – 1588	83
Σ_{16}PAH	**557–2731**	**2074**	**421–3245**	**1684**	**1875–22,405**	**11,752**	**3553–24,517**	**5501**	**234–22,082**	**1290**
9-FLO	<LOD – 41	33	<LOD – 33	<LOD	<LOD – 199	76	24–335	42	<LOD – 135	<LOD
9,10-AQ	<LOD – 127	43	<LOD – 98	69	33–785	152	59–2781	149	<LOD – 362	23
2-MAQ	<LOD – 61	30	<LOD – 42	<LOD	<LOD – 331	80	<LOD – 2197	74	33–3833	157
7,12-BaAQ	<LOD	<LOD	<LOD – 99	<LOD	<LOD – 810	100	<LOD – 1203	<LOD	<LOD – 998	<LOD
Σ_4OPAH	**60–251**	**128**	**23–254**	**143**	**68–2110**	**643**	**83–6516**	**318**	**54–5179**	**234**

<LOD = below method limit of detection.

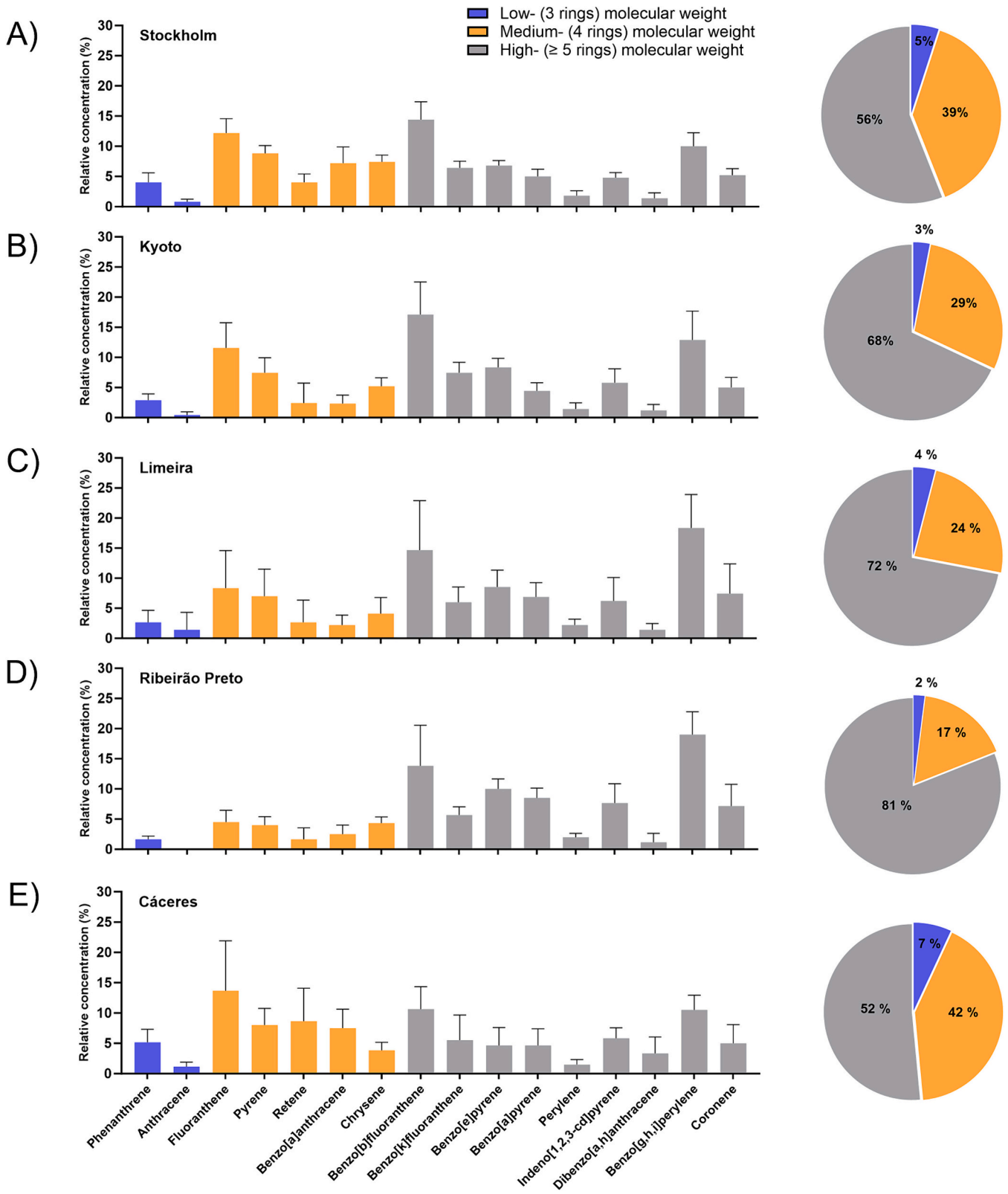

Fig. 2. Relative contribution of each PAH and of the groups low-molecular-weight (LMW-PAHs; 3 rings), medium-molecular weight (MMW-PAHs; 4 rings), and high-molecular-weight PAHs (HMW-PAHs; ≥ 5 rings) to total Σ_{16}PAH in $PM_{2.5}$ collected at (A) Stockholm, (B) Kyoto, (C) Limeira, (D) Ribeirão Preto and (E) Cáceres. Data show mean ± SD, n = 5–9.

Table 3
Concentration ranges and medians (ng m^{-3}) of the monosaccharide anhydrides (MAs) levoglucosan, mannosan and galactosan in the $PM_{2.5}$ samples collected in Stockholm, Kyoto, Limeira, Ribeirão Preto and Cáceres.

MAs (ng m^{-3})	Stockholm ($n = 5$)		Kyoto ($n = 9$)		Limeira ($n = 9$)		Ribeirão Preto ($n = 6$)		Cáceres ($n = 6$)	
	min–max	median	min–max	median	min–max	median	min–max	median	min–max	median
Levoglucosan (L)	<LOD - 127	70	<LOD – 105	65	142–1046	622	456–2069	1169	37–1899	213
Mannosan (M)	<LOD - 17	<LOD	<LOD – 27	<LOD	<LOD – 89	86	25–173	100	<LOD	<LOD
Galactosan (G)	<LOD	<LOD	<LOD	<LOD	<LOD – 61	57	14–128	67	<LOD - 200	<LOD
Σ_3MAs	**<LOD - 144**	**70**	**<LOD – 134**	**61**	**142–1190**	**661**	**495–2371**	**1336**	**37–2306**	**238**
L/M	<LOD - 8	<LOD	<LOD – 22	12	10–12	10	11–18	12	–	–
L/G	–	–	–	–	14–18	15	16–32	18	<LOD – 15	14

<LOD = below method limit of detection.

presented to give some indication about the type of biomass burned. The ratios of mannosan and galactosan reflect the relative proportions of mannose and galactose in hemicelluloses found across different plant species (Suciu et al., 2019). For instance, low L/M ratios (2–7) are often associated to softwood combustion, since softwoods contain a higher proportion of mannose units than hardwoods. In turn, higher L/M ratios (> 10) are mainly attributed to burning of hardwoods, grass and crop residues (Zhang et al., 2015). The ratio L/G is less discussed in the literature, but this ratio has been used to differentiate between combustion emission of leaves from wood (Schmidl et al., 2008).

The samples collected at Stockholm and Kyoto had the lowest concentrations of MAs, indicating lower input of PM from biomass burning at these sites compared to the Brazilian cities (Table 3). Here, the concentrations of levoglucosan found in Stockholm were similar to the ones reported by a recent study performed at a residential area near Stockholm during winter 2017 which detected up to 105 ng m^{-3} of levoglucosan and 14.2 ng m^{-3} of mannosan + galactosan in PM_{10} samples (Lim et al., 2022). In the same study, the L/M + G ratio suggested that domestic burning of hard and softwood for heating was the main emission source. Here, the L/M ratio of up to 8 indicated burning of softwood. In Kyoto, levoglucosan concentrations were comparable with those observed during the winter of 2014 in Moriguchi (18.4–110 ng m^{-3}), a city close to Kyoto (~45 km) with significant influence of automobile emissions (Ikemori et al., 2021). The L/M ratio of 12 indicated influence from combustion of hardwood and crop-residues. In Japan, the dominant source of levoglucosan has been reported as open burning of agricultural biomass and dry vegetation (Kumagai et al., 2010).

The Brazilian cities had the highest concentrations of MAs, with highest in Ribeirão Preto, followed by Limeira and Cáceres. The concentration ranges of levoglucosan, mannosan and galactosan found in the two former were higher than previously reported for TSP and PM_{10} samples collected during the dry season of several cities located inland of São Paulo State (Carvalho et al., 2023b; Caumo et al., 2016; Urban et al., 2014; Urban et al., 2012). Similar to $PM_{2.5}$ and PACs, Σ_3MA concentrations showed high variability in Cáceres samples, with a ~ 2 orders of magnitude difference between the minimum and maximum (Table 3).

The L/M ratios obtained in Limeira and Ribeirão Preto were ≥ 10, indicating combustion of hardwood, grass and crop residues. This was expected, given that softwoods (conifers) are relatively uncommon in these particular regions of Brazil, with a higher prevalence in the southern parts of the country. Ribeirão Preto and Limeira are located in the agro-industrial region of São Paulo state, the largest producer of sugarcane in Brazil. Despite the elimination of sugarcane manual harvesting preceded by fire, the state has experienced a substantial increase in the number of fires spots in 2020 and 2021 (6123 and 5469), compared to the average for the 9 previous years (3190) (INPE – Instituto Nacional de Pesquisas Espaciais, 2023). Moreover, biomass burning has been observed as the main source of several PACs in Ribeirão Preto, primarily due to land clearance in agriculture, accidental or criminal wild and crop fires (Scaramboni et al., 2024).

The L/G ratio of 14 found in Cáceres was similar to the value obtained by de Oliveira Alves et al. (2015) in a forest reserve site in the Amazon Basin (Porto Velho, L/G = 13.4), in accord with being located in the arc of deforestation. In contrast, mannosan was not detected, indicating that Savanna grass is also an important biofuel at this site, since it contains even less mannose than hardwoods (Engling et al., 2006).

3.4. Inorganic elements

Table 4 presents the concentrations of inorganic elements in $PM_{2.5}$ from the five studied cities. The Brazilian cities showed higher concentrations compared to Kyoto and Stockholm, with Limeira presenting the highest sum concentration (Σ_{15} elements), followed by Cáceres, Ribeirão Preto, Kyoto, and Stockholm. K and Fe were most abundant in Brazilian cities, while S and Fe were dominant in Stockholm, and S in Kyoto. Concentrations of Cr, Mn, Ni, Cu, and Pb in Stockholm aligned with previous studies (Johansson et al., 2009), while Fe, Ni, Cu, and Pb in Kyoto matched recent findings from Tokyo (Kaneyasu et al., 2020). The concentrations of As, V, Ni, and Cu found in Ribeirão Preto were similar to previous PM_{10} studies, except for Mn, Cd, and Pb which were ~ 10 times lower (Alves et al., 2019). The concentrations of Cáceres aligned with samples from Alta Floresta, a city located in the same state as Cáceres (Maenhaut et al., 2002).

WHO annual AQGs for Pb and Cd were not exceeded, indicating minimal health risks. Enrichment factors revealed Stockholm samples enriched with S, Cu, Se, and Cd, likely from local road traffic, while Kyoto showed similar enrichment, besides As and Pb (Fig. 3). Enrichment of Cu, Cd, and Pb has already been reported for fine PM samples from Kanazawa, Japan, and was related to vehicle brake wear (Cu) and combustion of coal and oil (Cd) and waste (Pb) (Wang et al., 2006). Limeira exhibited enrichment with P, S, Cu, As, Se, Ag, Cd, and Pb, associated with vehicular emissions and industrial sources (Canteras et al., 2013). Ribeirão Preto and Cáceres showed enrichment patterns reflecting local emission sources, including biomass burning in Cáceres. These differences shed light on variations in emission sources across cities.

3.5. Source identification

Positive Matrix Factorization (PMF) receptor model has been developed specifically for source apportionment of PM (Galvão et al., 2021; Reff et al., 2007). Substantial efforts were made here to find a stable model with meaningful physical interpretations, but without success. Although stable models were found with either a three- or four-factor solution, no meaningful interpretations could be made (not shown). We assume that this was due to the combination of relatively few samples (35 filters) with large variations of analyte concentrations (cf. Tables 2–4) as suggested by Galvão et al. (2021) and Henry et al. (1984). Besides that, source profiles at such different locations may differ, and combining all the studied cities data to develop a single model might not be appropriate. Therefore, we applied a combination of diagnostic PAH ratios (DRs), markers of biomass combustion, PCA and Spearman's correlations of the samples data in addition to the element

Table 4
Concentration ranges and medians (ng m^{-3}) of inorganic elements in the $PM_{2.5}$ samples collected in Stockholm, Kyoto, Limeira, Ribeirão Preto, and Cáceres.

Element (ng m^{-3})	Stockholm ($n = 5$)		Kyoto ($n = 9$)		Limeira ($n = 9$)		Ribeirão Preto ($n = 6$)		Cáceres ($n = 6$)	
	min–max	median	min–max	median	min–max	median	min–max	median	min–max	median
P	<LOD – 14.1	<LOD	0.75–20.6	8.8	<LOD – 84.7	20.9	<LOD – 3.1	<LOD	<LOD	<LOD
S	81.5–554	161	315–705	537	<LOD – 1181	195	<LOD – 65.5	15.3	<LOD – 334	155
K	<LOD	<LOD	<LOD - 383	47.8	<LOD – 2224	782	339–1658	703	<LOD – 15,517	719
Ca	<LOD	<LOD	<LOD – 88.7	<LOD	<LOD	<LOD	<LOD	<LOD	219–22,050	386
V	0.65–1.71	1.27	0.211–0.553	0.293	0.34–4.14	1.98	0.66–1.84	1.37	0.088–0.835	0.399
Cr	1.10–2.45	1.45	0.66–1.63	1.03	1.05–4.42	1.66	0.47–2.26	1.20	<LOD	<LOD
Mn	3.46–9.67	7.46	3.71–8.94	6.21	6.56–24.0	11.7	3.28–6.39	4.89	0.36–8.49	1.73
Fe	275–643	579	112–257	171	204–1558	780	207–603	395	31.2–357	151
Ni	0.39–1.74	0.66	0.53–1.04	0.77	0.11–2.02	0.62	0.14–0.76	0.23	<LOD	<LOD
Cu	3.82–16.8	7.38	<LOD – 4.90	2.79	12.6–163	73.6	12.2–65.1	28.6	27.1–689	109
As	0.06–0.20	0.16	0.38–0.93	0.68	0.24–1.25	0.62	0.16–0.85	0.54	<LOD – 0.71	0.16
Se	0.04–0.20	0.10	0.36–0.80	0.68	0.21–1.70	0.72	0.05–0.39	0.26	0.01–0.73	0.09
Ag	<LOD – 0.007	0.001	0.02–0.19	0.05	0.05–0.21	0.10	0.01–0.03	0.02	0.02–0.26	0.06
Cd	0.01–0.08	0.02	0.04–0.20	0.17	0.07–0.66	0.30	0.07–0.20	0.12	0.02–0.51	0.05
Pb	0.33–2.56	0.60	2.74–7.56	5.44	4.94–19.8	6.55	1.47–4.68	3.12	0.29–17.8	0.83
Σ_{15} elements	**390–1231**	**759**	**508–1272**	**825**	**465–3974**	**1703**	**577–2294**	**1206**	**131–16,083**	**1560**

<LOD = below method limit of detection.

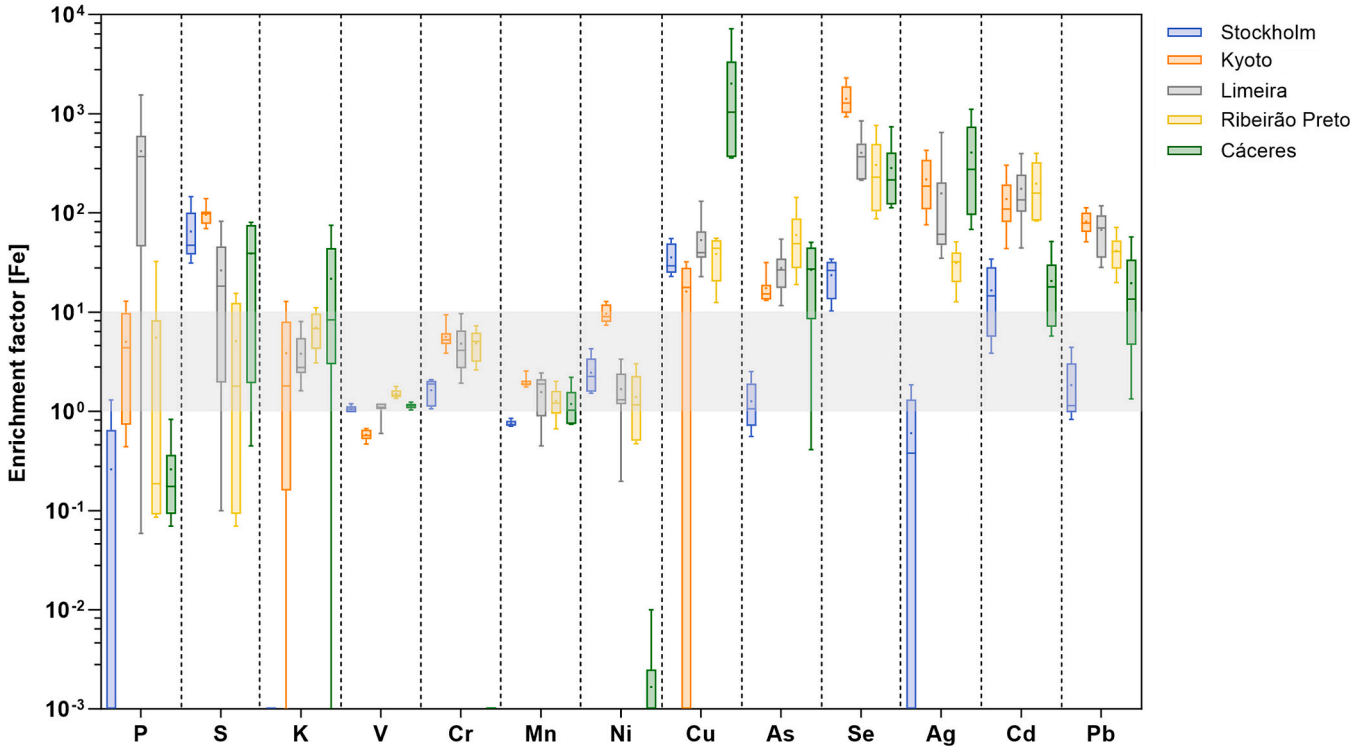

Fig. 3. Enrichment factors (EF) of measured elements using Fe as reference compound. The box range indicates the 25th and 75th percentile, the whiskers from min to max, and the line is the distribution median. The mean values are shown as dots. The shaded area corresponds to $1 < EF < 10$. EF values close to 1 is considered crustal or as natural, $1 < EF < 10$ is considered non-enriched, $10 < EF < 100$ is moderately enriched, and $EF > 100$ is highly enriched (da Silva et al., 2019; Taner et al., 2013).

EFs presented above to assess the most likely emission sources.

3.5.1. Diagnostic ratios (DRs)

DRs were calculated to obtain semi-quantitative insights into PAH emission sources (Table 5). Since PAHs are emitted from a range of sources and due to their atmospheric reactivity, their profiles can be modified as a function of distance from the source and meteorological conditions, these ratios should be interpreted with caution (Katsoyiannis and Breivik, 2014; Wu et al., 2021). To minimize the effect of differences in atmospheric persistence and gas-particle partitioning, the DRs calculated in this work did not include LMW PAHs, which are mainly present in the gas-phase and are more reactive (Kim et al., 2013).

Across all five cities, the ratios of Flt/(Flt + Pyr) were above 0.4, and the ratios of BaA/(BaA + Chr) and InP/(InP + BPer) were above 0.2, thus consistently pointing towards the prevalence of pyrogenic over petrogenic sources (Yunker et al., 2002). This was expected because petrogenic sources are more often related to PAH deposition in sediments from petroleum refining activities and oil spills than pyrogenic sources, which are dominant in air samples (De La Torre-Roche et al., 2009; Tobiszewski and Namieśnik, 2012). The ratios Flt/(Flt + Pyr) and InP/(InP + BPer) indicated that the pyrogenic sources were a mixture of vehicle emission and biomass combustion. Low Ret/(Ret + Chr) ratios

Table 5
Diagnostic ratios (DRs) calculated for polycyclic aromatic hydrocarbons (PAHs) determined in the $PM_{2.5}$ samples collected in Stockholm, Kyoto, Limeira, Ribeirão Preto, and Cáceres. The DRs used as source indicators were retrieved from Tobiszewski and Namieśnik (2012) and references therein. Data are presented as range and median (in parenthesis).

DR	Stockholm ($n = 5$)	Kyoto ($n = 9$)	Limeira ($n = 9$)	Ribeirão Preto ($n = 6$)	Cáceres ($n = 6$)
Flt / (Flt + Pyr)[a]	0.52–0.62 (0.59)	0.53–0.66 (0.60)	0.43–0.61 (0.54)	0.43–0.56 (0.54)	0.50–0.70 (0.60)
BaA / (BaA + Chr)[b]	0.43–0.58 (0.47)	0.09–0.47 (0.37)	0.21–0.49 (0.35)	0.34–0.50 (0.44)	0.59–0.76 (0.64)
InP / (InP + BPer)[c]	0.24–0.41 (0.34)	0.08–0.44 (0.36)	0.08–0.41 (0.30)	0.04–0.42 (0.28)	0.30–0.42 (0.37)
BaP / BPer[d]	0.25–0.71 (0.60)	0.08–0.56 (0.44)	0.19–0.68 (0.35)	0.13–0.58 (0.47)	0.16–0.67 (0.45)
BaP / (BaP + BeP)[e]	0.31–0.49 (0.45)	0.23–0.41 (0.35)	0.34–0.54 (0.45)	0.38–0.51 (0.47)	0.39–0.68 (0.52)
Ret / (Ret + Chr)[f]	0.25–0.47 (0.32)	0.09–0.71 (0.17)	0.05–0.61 (0.19)	0.07–0.58 (0.29)	0.46–0.84 (0.68)

[a] < 0.4: petrogenic; 0.4–0.5: fossil fuel combustion; > 0.5: grass, wood, and coal combustion.
[b] < 0.2: petrogenic;> 0.35: pyrogenic.
[c] < 0.2: petrogenic; 0.2–0.5: petroleum combustion; > 0.5: grass, wood, and coal combustion.
[d] < 0.6: non-traffic emissions; > 0.6: traffic emissions.
[e] < 0.5: aged particles; > 0.5: fresh particles.
[f] 0.15–0.50: petroleum combustion; 0.30–0.45 coal combustion; ~1: wood burning.

have been related to coal and petroleum while a value around 1 has been associated with wood burning (Yan et al., 2005). The highest median of this DR was obtained for Cáceres (0.68), which agrees with the observed enrichment of K presented above. The BaP/BPer ratio is associated with non-traffic (< 0.6) or traffic-related emissions (> 0.6) (Katsoyiannis et al., 2007). The highest value was obtained for Stockholm (0.60) in accordance with its close location to a highway and the observed enrichment of several elements related to road traffic.

Based on differences in atmospheric reactivity, the BaP/(BaP + BeP) ratio can be used to estimate the aging of particulate matter (Oliveira et al., 2011). This DR indicated fresh PM emissions in Cáceres > Ribeirão Preto > Limeira > Stockholm and more aged particles in Kyoto. This corroborated with the proximity of fire spots in Cáceres and long-range trajectories of air masses coming from China and South Korea to Kyoto (Figs. S2 and S5). All DR analysis underscores biomass burning and vehicular emissions as the main PAH sources across the five cities.

3.5.2. Markers of biomass burning

Chemical markers (e.g., K, levoglucosan, mannosan, galactosan, and retene), diagnostic ratios (e.g., K^+/EC, OC/EC, ratios of PAHs), and specific target particles (e.g., soot, tarballs, crystal KCl particles) are commonly used to specifically trace biomass burning and support source apportionment of biomass burning emissions (Chen et al., 2017; Simoneit, 2002). It is important to note that while these markers can provide valuable information about the presence and contribution of biomass burning to $PM_{2.5}$, their interpretation often requires consideration of other factors such as local emission sources, meteorological conditions, and the potential for secondary aerosol formation (Lee et al., 2021). Fig. 4A shows levels of the biomass-burning markers retene, levoglucosan, and K in the five cities, and Fig. 4B–D the backward air mass trajectories for the samples with the highest levels of these markers (filters RP02, C04, and L10). The general observation of elevated concentrations of these markers in Limeira, Ribeirão Preto, and Cáceres reflected a higher biomass burning input to these areas than Stockholm and Kyoto, presumably due to extensive wild and crop fires.

In addition to local fires, the backward air mass trajectory analysis revealed an influence of long-range transport of smoke from wildfires in the Amazon region and in the Brazilian savanna region (Cerrado) (Fig. 4B-D). The smoke of these fires was also clearly depicted in satellite images. In the Amazon, fire emissions have increased in recent years due to escalating deforestation rates, and the Cerrado biome has also had a substantial increase in the number of wildfire events mostly due to land use (Cobelo et al., 2023; Silva et al., 2023). The smoke produced during such episodes extends wildfire impacts far beyond the immediate vicinity of the flames, potentially increasing mortality risks and $PM_{2.5}$-related health effects (Butt et al., 2021; Ye et al., 2022; Yu et al., 2022).

3.5.3. PCA and Spearman's correlations

PCA was performed to reduce data dimensionality, identify statistical patterns and major sources of the measured air pollutants. The extraction of 4 components was able to explain 77% of the data variability, in which the first component (PC1) explained 48% and the second component (PC2) explained 16% of the variability (Table S5). The scores plot of PC1 versus PC2 (Fig. 5A) indicated similarity between samples from Stockholm and Kyoto, while the samples from the Brazilian cities were more scattered in the plot.

PC1 showed high loadings for PAHs (0.67–0.95), levoglucosan (0.81), and OPAHs (0.62–0.87) (Fig. 5B, Table S5). In addition, most of the samples with elevated concentrations of biomass burning markers (Fig. 4A) clustered together and were strongly associated with PC1 (Fig. 5A). Notably, K was separated from the other inorganic elements and ratter clustered with the biomass burning markers and PACs (Fig. 5B). Thus, PC1 likely represented biomass-burning sources. Most samples from Brazilian cities showed higher loadings for PC1 compared to Stockholm and Kyoto (Fig. 5A), which reinforced the strong influence of biomass burning in these cities. Spearman's correlations also indicated that the Brazilian cities had substantial input of $PM_{2.5}$ from biomass burning. In Limeira, Σ_3MAs significantly correlated with Σ_{16}PAH and $PM_{2.5}$ ($r_s = 0.70–0.87$; $p < 0.05$) (Fig. S7), while in Ribeirão Preto Σ_3MA significantly correlated more strongly with HMW PAHs, Σ_4OPAH and $PM_{2.5}$ ($r_s = 0.83–1.00$; $p < 0.05$) (Fig. S8). In Cáceres, Ret significantly correlated with $PM_{2.5}$ and all LMW PAHs, indicating wood burning as an important source ($r_s = 0.83–1.00$; $p < 0.05$) (Fig. S9).

However, our data suggested that biomass burning was not the only major source of $PM_{2.5}$ in Limeira which displayed a more scattered arrangement in the scores plot (Fig. 4A). Limeira samples L08, L06, and L03 were separated from the others and associated with PC2 which had high loadings for most inorganic elements, such as S, V, Cr, Mn, Fe, Ni, As, Se, Cd, and Pb (0.50–0.85) (Table S5), indicating traffic emissions (exhaust and non-exhaust) and industrial sources. This aligns with the complexity and variability of emission sources previously reported in Limeira, encompassing factors such as vehicular traffic, industrial discharges, in addition to biomass burning (Maselli et al., 2020; Pozza et al., 2023).

In contrast to Limeira, Stockholm $PM_{2.5}$ levels strongly correlated with Σ_{16}PAH, Σ_4OPAH and Σ_{15}elements ($r_s = 0.90–1.00$; $p < 0.05$), indicating a unique major source for organic and inorganic compounds (Fig. S10). The elements S, Cu, V, and Pb significantly correlated with HMW PAHs ($r_s = 0.90–1.00$; $p < 0.05$) and supported the DRs that indicated traffic emissions as the most important source of the $PM_{2.5}$ at this site, while biomass burning seems to be a minor source. This is further in agreement with a recent study that identified vehicle exhaust emissions as the main source of PACs in PM_{10} at this site during the winter (Sadiktsis et al., 2023). In Kyoto, Σ_{16}PAH and Σ_4OPAH had a strong correlation ($r_s = 0.95$; $p = 0.0003$) while in Stockholm such a significant correlation was not observed ($r_s = 0.70$; $p = 0.23$) (Fig. S10). This may indicate a similar source and/or that OPAHs were formed from oxidation of the parent PAHs in the atmosphere. For Kyoto, this latter scenario is supported by the BaP/(BaP + BeP) ratio and the backward air mass trajectories that mostly came from mainland China (Table 5; Fig. S3). In addition, the high concentration of S found in Kyoto samples indicate emissions from coal and oil combustion, which represent 66% of the total energy supply in Japan and 79% in China (IEA –

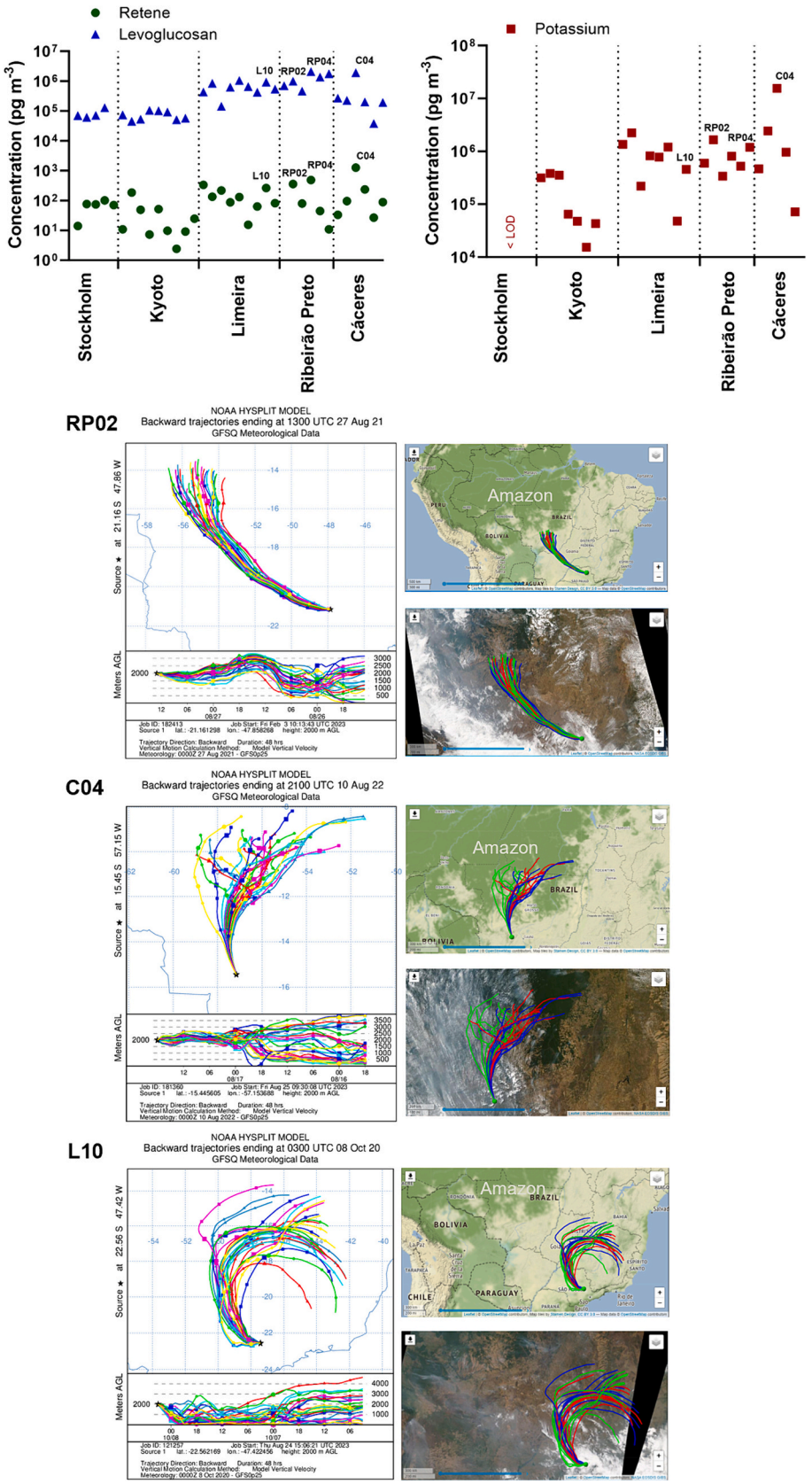

Fig. 4. Markers of biomass burning. A) Levels of retene, levoglucosan, and K. Filters displaying the highest concentrations of these markers were labeled. Backward trajectories and satellite photos of the sampling point in B) Ribeirão Preto (RP02), C) Cáceres (C04), and D) Limeira (L10) indicating the convergence of air masses coming from the Amazon rainforest and the Brazilian savanna to these three cities. The colors in trajectories (B—D) represent different offsetting of meteorological data and the symbols are spaced at 6-h intervals up to 48 h. See Figs. S2–S6 for backward trajectories for other filters.

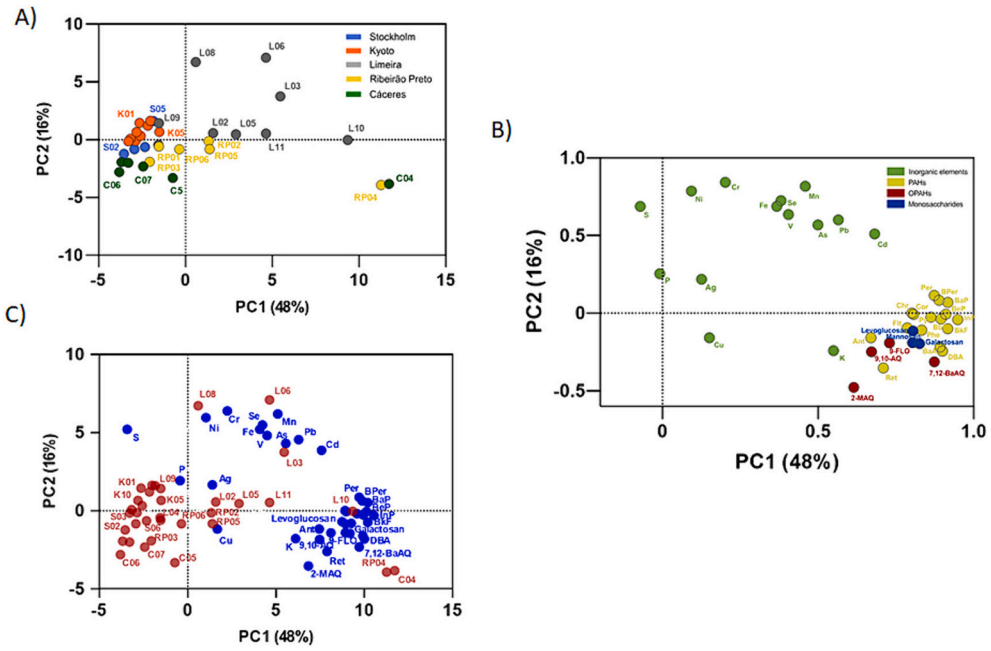

Fig. 5. Principal component analysis of PAC, inorganic element, and monosaccharide anhydride data (pg m^{-3}) from the five sites (37 variables and 35 samples). A) Scores plot of individual filters, B) Loadings plot of analytes and C) Combined scores and loadings plots.

International Energy Agency, 2022). The MAs and K did not correlate significantly with any organic or inorganic compounds determined (Fig. S11), which together with the DRs suggested that biomass burning is not a major emission source in Kyoto. Taken together, the combination of DRs, EFs and correlation analyses indicated that the main sources of Kyoto $PM_{2.5}$ were waste burning, fossil fuel combustion, and long-range transport.

Although PC1 likely represented biomass burning emissions, the highest loadings in PC3 were of K (0.67) and Ret (0.46) suggesting a more complex pattern of emission sources (Table S5). Similarly, MAs overall correlated strongly with each other ($0.90 < r_s < 0.95$), but only moderately with K ($0.60 < r_s < 0.75$) and weakly with Ret ($0.37 < r_s < 0.40$) (Fig. S12). These differences could indicate additional emission sources to biomass burning for K and Ret. The former is also associated with soil dust, coal combustion particles, and sea salt (Rahman et al., 2020). Significant input of soil dust and sea salt is not expected in these samples, since they are more relevant as sources of coarse particles, not $PM_{2.5}$. However, K is also emitted as a biogenic salt by the biota in the Amazon rainforest that is found in fine PM (Pöhlker et al., 2012). Notably, samples from Cáceres, which is impacted by Amazon emissions from biomass burning or biogenic origin (Fig. 4C), had the highest PC3 loadings (Fig. S13), and the highest EF for K (Fig. 3). Moreover, de Oliveira Alves et al. (2015) found that biomass burning was not the only source of Ret in the Amazon region, but also emitted from coal combustion. Taken together, PC3 likely represents mixed sources, including biogenic emissions and coal combustion. PC4 explained 5.9% of the total variance and had low loadings, so no specific source could be associated with this component.

All approaches used to assess emission sources yielded insights into the main sources of ambient $PM_{2.5}$ in our studies areas. Nevertheless, it is important to recognize that these sources exhibit significant temporal and spatial variability, as evidenced by the dynamic emission profiles reflected in the different concentrations of chemical species among the samples.

4. Conclusions

This cross-continental study provided valuable insights into $PM_{2.5}$ composition and source contributions, emphasizing the impact of various emission sources on air quality among the five studied cities.

Diagnostic ratios suggested prevalence of pyrogenic sources of PAHs, mainly biomass burning and vehicular emissions, across the five cities. Fresh PM emissions observed in Cáceres corroborated with the proximity of fire spots and more aged particles in Kyoto with the long-range trajectories of air masses coming from China and South Korea.

Biomass burning was associated with 48% of the data variance, and most samples from Limeira, Ribeirão Preto and Cáceres showed higher loadings for the biomass burning component compared to Stockholm and Kyoto. This indicated a strong influence of this source in the Brazilian cities, likely attributable to widespread Amazon and Cerrado wildfires and local fires.

Traffic emissions (exhaust and non-exhaust) and industrial sources were associated with 16% of the data variance. Inorganic elements analysis showed that in Stockholm, traffic emissions were the most important source of $PM_{2.5}$, while in Kyoto a combination of traffic, waste combustion, and long-range transport were the main contributors. Brazilian cities also showed a notable influence of traffic and industrial sources, especially in Limeira, besides the evident biomass burning.

Despite regional disparities, Stockholm and the three Brazilian cities exhibited $PM_{2.5}$ levels above WHO short-term guidelines, with the Brazilian cities experiencing the highest air pollution. Brazilian cities exhibited the highest levels of total polycyclic aromatic compounds (1.5–12.4 ng m^{-3}), monosaccharide anhydrides (238–1336 ng m^{-3}), and inorganic elements (1206–1703 ng m^{-3}). Indeed, the health impact of air pollution in Brazil is well established, with clear correlations between increased PM emission from wildfires and hospital admissions and mortality. Our results support the importance of improving the air quality especially during the emission-intense winter/dry season to reach air quality standards and limit human health effects from air pollution.

CRediT authorship contribution statement

Caroline Scaramboni: Conceptualization, Formal analysis, Investigation, Methodology, Writing – original draft, Writing – review & editing. **Camila Novais Farias:** Investigation, Methodology, Writing – original draft. **Pérola de Castro Vasconcellos:** Resources, Writing – review & editing. **Michael Levi:** Investigation, Methodology, Writing –

review & editing. **Ioannis Sadiktsis:** Investigation, Methodology, Resources, Writing – review & editing, Conceptualization. **Simone Andréa Pozza:** Investigation, Methodology, Writing – review & editing. **Gisela de Aragão Umbuzeiro:** Writing – review & editing. **Tetsushi Watanabe:** Investigation, Methodology, Writing – review & editing. **Poliany Cristiny de Oliveira Rodrigues:** Investigation, Methodology. **Adriana Grandis:** Investigation, Methodology, Writing – review & editing. **Débora Pagliuso:** Investigation, Methodology, Writing – review & editing. **Marcos Silveira Buckeridge:** Resources. **Maria Lucia Arruda Moura Campos:** Writing – review & editing. **Maria Kippler:** Resources, Writing – review & editing. **Kristian Dreij:** Formal analysis, Funding acquisition, Resources, Supervision, Writing – original draft, Writing – review & editing, Conceptualization. **Marcos Felipe de Oliveira Galvão:** Conceptualization, Formal analysis, Funding acquisition, Investigation, Methodology, Resources, Supervision, Writing – original draft, Writing – review & editing.

Declaration of competing interest

The authors declare that they have no known competing financial interests or personal relationships that could have appeared to influence the work reported in this paper.

Data availability

Data will be made available on request.

Acknowledgments

This research was funded by the Swedish Research Council Formas (grant number 2019-00582), by a Joint Brazilian-Swedish Research Collaboration funded by the CAPES, Brazil, and STINT, Sweden (grant numbers BR2019–8515 and 88887.642068/2021–00), by CNPq (CNPq 301503/2018-4) and FAPESP (Metroclima 2016/18438-0). C.S. was supported by FAPESP (#2018/17931-0). C.N.F. was supported by CAPES (PROEX-88887.624108/2021-00) and CNPq (140541/2023-3). A.G. was supported by FAPESP (2019/13936-0). M.F.O.G was supported by Formas (grant number 2022-01484). We thank Captain Leandro Alves (Fire Department of Cáceres) and Marcelo de Andrade (Chico Mendes Institute for Biodiversity Conservation, ICMBio) for their support with the sampling campaign in Cáceres.

Appendix A. Supplementary data

Supplementary data to this article can be found online at https://doi.org/10.1016/j.atmosres.2024.107423.

References

Alves, R.I.S., Machado, G.P., Zagui, G.S., Bandeira, O.A., Santos, D.V., Nadal, M., Sierra, J., Domingo, J.L., Segura-Muñoz, S.I., 2019. Metals risk assessment for children's health in water and particulate matter in a southeastern Brazilian city. Environ. Res. 177, 108623 https://doi.org/10.1016/j.envres.2019.108623.

Bi, J., Carmona, N., Blanco, M.N., Gassett, A.J., Seto, E., Szpiro, A.A., Larson, T.V., Sampson, P.D., Kaufman, J.D., Sheppard, L., 2022. Publicly available low-cost sensor measurements for PM2.5 exposure modeling: guidance for monitor deployment and data selection. Environ. Int. 158, 106897 https://doi.org/10.1016/J.ENVINT.2021.106897.

Boström, C.E., Gerde, P., Hanberg, A., Jernström, B., Johansson, C., Kyrklund, T., Rannug, A., Törnqvist, M., Victorin, K., Westerholm, R., 2002. Cancer risk assessment, indicators, and guidelines for polycyclic aromatic hydrocarbons in the ambient air. Environ. Health Perspect. 110, 451–488. https://doi.org/10.1289/ehp.110-1241197.

Bousiotis, D., Allison, G., Beddows, D.C.S., Harrison, R.M., Pope, F.D., 2023. Towards comprehensive air quality management using low-cost sensors for pollution source apportionment. NPJ Clim. Atmos. Sci. 6, 1–10. https://doi.org/10.1038/s41612-023-00424-0.

Butt, E.W., Conibear, L., Knote, C., Spracklen, D.V., 2021. Large air quality and public health impacts due to Amazonian deforestation fires in 2019. GeoHealth 5, 1–16. https://doi.org/10.1029/2021GH000429.

Calvo, A.I., Alves, C., Castro, A., Pont, V., Vicente, A.M., Fraile, R., 2013. Research on aerosol sources and chemical composition: past, current and emerging issues. Atmos. Res. 120–121, 1–28. https://doi.org/10.1016/j.atmosres.2012.09.021.

Canteras, F.B., Moreira, S., de Faria, B.F., 2013. Study of main and signature sources of particulate matter pollutants in Limeira City (Brazil) using SR-TXRF. X-Ray Spectrom. 42, 290–298. https://doi.org/10.1002/xrs.2468.

Carvalho, J.S., Ferraz, G.M., Betim, H.L.I., Nascimento, R.K.S., Scaramboni, C., Urban, R. C., 2023a. What Can We Learn about Improvements in Air Quality During the COVID-19 Pandemic? A Case Study in Four Cities Located in the Same State but with Different Emission Profiles. J. Braz. Chem. Soc. e-20230110. https://doi.org/10.21577/0103-5053.20230110.

Carvalho, J.S., Nascimento, R.K.S., Ferreira, J.V.F.R., da Rosa, N.L.C., Grosseli, G.M., Fadini, P.S., Urban, R.C., 2023b. Source apportionment and health impact assessment of atmospheric particulate matter in the city of São Carlos, Brazil. Chemosphere 138450. https://doi.org/10.1016/j.chemosphere.2023.138450.

Caumo, S.E.S., Claeys, M., Maenhaut, W., Vermeylen, R., Behrouzi, S., Safi Shalamzari, M., Vasconcellos, P.C., 2016. Physicochemical characterization of winter PM10 aerosol impacted by sugarcane burning from São Paulo city, Brazil. Atmos. Environ. 145, 272–279. https://doi.org/10.1016/j.atmosenv.2016.09.046.

CETESB - – Companhia Ambiental do Estado de São Paulo, 2020. Relatório de Qualidade do Ar no Estado de São Paulo-2020. Available at: https://cetesb.sp.gov.br/ar/wp-content/uploads/sites/28/2021/05/Relatorio-de-Qualidade-do-Ar-no-Estado-de-Sao-Paulo-2020.pdf. Accessed on 01 November 2023.

CETESB – Companhia Ambiental do Estado de São Paulo, 2021. Relatório Qualidade do Ar no Estado de São Paulo - 2021. Available at: https://cetesb.sp.gov.br/ar/wp-content/uploads/sites/28/2022/10/Relatorio-de-Qualidade-do-Ar-no-Estado-de-Sao-Paulo-2021.pdf. Accessed on 01 November 2023.

Chen, J., Li, C., Ristovski, Z., Milic, A., Gu, Y., Islam, M.S., Wang, S., Hao, J., Zhang, H., He, C., Guo, H., Fu, H., Miljevic, B., Morawska, L., Thai, P., Lam, Y.F., Pereira, G., Ding, A., Huang, X., Dumka, U.C., 2017. A review of biomass burning: emissions and impacts on air quality, health and climate in China. Sci. Total Environ. 579, 1000–1034. https://doi.org/10.1016/J.SCITOTENV.2016.11.025.

Cobelo, I., Jablinski, F., Borge, R., Roig, H.L., Adams, M., Amini, H., Koutrakis, P., Weeberb, J.R., 2023. The impact of wildfires on air pollution and health across land use categories in Brazil over a 16-year period. Environ. Res. 224, 115522 https://doi.org/10.1016/j.envres.2023.115522.

da Silva, K.K., Duarte, F.T., Rodrigues Matias, J.N., Morais Medeiros Dias, S.A., de Duarte, E.S.F., Cunha da Silva Soares, C.G., Hoelzemann, J.J., de Oliveira Galvão, M. F., 2019. Physico-chemical properties and genotoxic effects of air particulate matter collected from a complex of ceramic industries. Atmos. Pollut. Res. 10, 597–607. https://doi.org/10.1016/j.apr.2018.11.001.

de Coringa, E.A.O., Couto, E.G., Torrado, P.V., 2014. Geoquímica de solos do pantanal norte, Mato Grosso. Rev. Bras. Ciência do Solo 38, 1784–1793. https://doi.org/10.1590/s0100-06832014000600013.

De La Torre-Roche, R.J., Lee, W., Campos-díaz, S.I., 2009. Soil-borne polycyclic aromatic hydrocarbons in El Paso, Texas: analysis of a potential problem in the United States / Mexico border region, 163, 946–958. https://doi.org/10.1016/j.jhazmat.2008.07.089.

de Oliveira Alves, N., Matos Loureiro, A.L., dos Santos, F.C., Nascimento, K.H., Dallacort, R., de Castro Vasconcellos, P., de Souza Hacon, S., Artaxo, P., de Medeiros, S.R.B., 2011. Genotoxicity and composition of particulate matter from biomass burning in the eastern Brazilian Amazon region. Ecotoxicol. Environ. Saf. 74, 1427–1433. https://doi.org/10.1016/j.ecoenv.2011.04.007.

de Oliveira Alves, N., De Souza Hacon, S., De Oliveira Galvão, M.F., Simões Peixotoc, M., Artaxo, P., De Castro Vasconcellos, P., De Medeiros, S.R.B., 2014. Genetic damage of organic matter in the Brazilian Amazon: a comparative study between intense and moderate biomass burning. Environ. Res. 130, 51–58. https://doi.org/10.1016/j.envres.2013.12.011.

de Oliveira Alves, N., Brito, J., Caumo, S., Arana, A., de Souza Hacon, S., Artaxo, P., Hillamo, R., Teinilä, K., Batistuzzo de Medeiros, S.R., de Castro Vasconcellos, P., 2015. Biomass burning in the Amazon region: aerosol source apportionment and associated health risk assessment. Atmos. Environ. 120, 277–285. https://doi.org/10.1016/j.atmosenv.2015.08.059.

de Oliveira Galvão, M.F., de Alves, N.O., Ferreira, P.A., Caumo, S., de Castro Vasconcellos, P., Artaxo, P., de Souza Hacon, S., Roubicek, D.A., Batistuzzo de Medeiros, S.R., 2018. Biomass burning particles in the Brazilian Amazon region: mutagenic effects of nitro and oxy-PAHs and assessment of health risks. Environ. Pollut. 233, 960–970. https://doi.org/10.1016/j.envpol.2017.09.068.

de Oliveira, I.N., de Oliveira, B.F.A., da Silveira, I.H., Machado, L.M.G., Villardi, J.W.R., Ignotti, E., 2023. Air pollution from forest burning as environmental risk for millions of inhabitants of the Brazilian Amazon: an exposure indicator for human health. Cad. Saude Publ. 39, e00131422 https://doi.org/10.1590/0102-311XEN131422.

Elmgren, M., Burman, L., 2020. Fordonssammansättning Kopplat Till HBEFA 4.1 vid E4/E20 Hallunda, Samt Hastighet- Och Trafikflödesprofiler. SLB Report 37.

Engling, G., Carrico, C.M., Kreidenweis, S.M., Collett, J.L., Day, D.E., Malm, W.C., Lincoln, E., Min Hao, W., Iinuma, Y., Herrmann, H., 2006. Determination of levoglucosan in biomass combustion aerosol by high-performance anion-exchange chromatography with pulsed amperometric detection. Atmos. Environ. 40, 299–311. https://doi.org/10.1016/j.atmosenv.2005.12.069.

Fadigas, F.D.S., Do Amaral Sobrinho, N.M.B., Mazur, N., Cunha Dos Anjos, L.H., 2006. Estimation of reference values for cadmium, cobalt, chromium, copper, nickel, lead, and zinc in Brazilian soils. Commun. Soil Sci. Plant Anal. 37, 945–959. https://doi.org/10.1080/00103620600583885.

Galvão, E.S., de Cassia Feroni, R., D'Azeredo Orlando, M.T., 2021. A review of the main strategies used in the interpretation of similar chemical profiles yielded by receptor

models in the source apportionment of particulate matter. Chemosphere 269, 128746. https://doi.org/10.1016/j.chemosphere.2020.128746.
Gonçalves, C., Rienda, I.C., Pina, N., Gama, C., Nunes, T., Tchepel, O., Alves, C., 2021. Pm10-bound sugars: chemical composition, sources and seasonal variations. Atmosphere (Basel) 12. https://doi.org/10.3390/atmos12020194.
Henry, R.C., Lewis, C.W., Hopke, P.K., Williamson, H.J., 1984. Review of receptor model fundamentals. Atmos. Environ. 18, 1507–1515. https://doi.org/10.1016/0004-6981(84)90375-5.
Hites, R.A., 2019. correcting for censored environmental measurements. Environ. Sci. Technol. 53, 11059–11060. https://doi.org/10.1021/acs.est.9b05042.
Hvidtfeldt, U.A., Severi, G., Andersen, Z.J., et al., 2021. Long-term low-level ambient air pollution exposure and risk of lung cancer – a pooled analysis of 7 European cohorts. Environ. Int. 146 https://doi.org/10.1016/j.envint.2020.106249.
IBGE - Instituto Brasileiro de Geografia e Estatítisca, 2022. Panorama das Cidades. Available at: https://cidades.ibge.gov.br/brasil/sp/ribeirao-preto/panorama. Accessed on 01 November 2023.
Idowu, O., Semple, K.T., Ramadass, K., O'Connor, W., Hansbro, P., Thavamani, P., 2019. Beyond the obvious: Environmental health implications of polar polycyclic aromatic hydrocarbons. Environ. Int. 123, 543–557. https://doi.org/10.1016/j.envint.2018.12.051.
IEA – International Energy Agency, 2022. Overview of Energy System 2022. Available at. https://www.iea.org. Accessed on 07 March 2024.
Ikemori, F., Uranishi, K., Asakawa, D., Nakatsubo, R., Makino, M., Kido, M., Mitamura, N., Asano, K., Nonaka, S., Nishimura, R., Sugata, S., 2021. Source apportionment in PM2.5 in Central Japan using positive matrix factorization focusing on small-scale local biomass burning. Atmos. Pollut. Res. 12, 162–172. https://doi.org/10.1016/j.apr.2021.01.006.
INPE – Instituto Nacional de Pesquisas Espaciais, 2023. Monitoring of Active Fire Spots by States. Portal Do Programa Queimadas Do INPE. Available at: http://www.inpe.br/queimadas/portal/estatistica_estados.
Jandacka, D., Durcanska, D., Cibula, R., 2022. Concentration and inorganic elemental analysis of particulate matter in a road tunnel environment (Žilina, Slovakia): contribution of non-exhaust sources. Front. Environ. Sci. 10, 1–17. https://doi.org/10.3389/fenvs.2022.952577.
Jarvis, I.W.H., Dreij, K., Mattsson, Å., Jernström, B., Stenius, U., 2014. Interactions between polycyclic aromatic hydrocarbons in complex mixtures and implications for cancer risk assessment. Toxicology 321, 27–39. https://doi.org/10.1016/j.tox.2014.03.012.
Johansson, C., Norman, M., Burman, L., 2009. Road traffic emission factors for heavy metals. Atmos. Environ. 43, 4681–4688. https://doi.org/10.1016/j.atmosenv.2008.10.024.
Kaneyasu, N., Ishidoya, S., Terao, Y., Mizuno, Y., Sugawara, H., 2020. Estimation of PM2.5 emission sources in the Tokyo metropolitan area by simultaneous measurements of particle elements and oxidative ratio in air. ACS Earth Space Chem. 4, 297–304. https://doi.org/10.1021/acsearthspacechem.9b00314.
Katsoyiannis, A., Breivik, K., 2014. Model-based evaluation of the use of polycyclic aromatic hydrocarbons molecular diagnostic ratios as a source identification tool. Environ. Pollut. 184, 488–494. https://doi.org/10.1016/J.ENVPOL.2013.09.028.
Katsoyiannis, A., Terzi, E., Cai, Q.Y., 2007. On the use of PAH molecular diagnostic ratios in sewage sludge for the understanding of the PAH sources. Is this use appropriate? Chemosphere 69, 1337–1339. https://doi.org/10.1016/j.chemosphere.2007.05.084.
Kelly, F.J., Fussell, J.C., 2012. Size, source and chemical composition as determinants of toxicity attributable to ambient particulate matter. Atmos. Environ. 60, 504–526. https://doi.org/10.1016/j.atmosenv.2012.06.039.
Kim, K.H., Jahan, S.A., Kabir, E., Brown, R.J.C., 2013. A review of airborne polycyclic aromatic hydrocarbons (PAHs) and their human health effects. Environ. Int. 60, 71–80. https://doi.org/10.1016/j.envint.2013.07.019.
Kippler, M., Gyllenhammar, I., Glynn, A., Levi, M., Lignell, S., Berglund, M., 2021. Total mercury in hair as biomarker for methylmercury exposure among women in Central Sweden– a 23 year long temporal trend study. Environ. Pollut. 268, 115712 https://doi.org/10.1016/j.envpol.2020.115712.
Kumagai, K., Iijima, A., Shimoda, M., Saitoh, Y., Kozawa, K., Hagino, H., Sakamoto, K., 2010. Determination of dicarboxylic acids and levoglucosan in fine particles in the kanto plain, Japan, for source apportionment of organic aerosols. Aerosol Air Qual. Res. 10, 282–291. https://doi.org/10.4209/aaqr.2009.11.0075.
Lee, G., Lee, Y.G., Jeong, E., Ho, C.H., 2021. Roles of meteorological factors in inter-regional variations of fine and coarse PM concentrations over the Republic of Korea. Atmos. Environ. 264, 118706 https://doi.org/10.1016/j.atmosenv.2021.118706.
Liang, L., Gong, P., 2020. Urban and air pollution: a multi-city study of long-term effects of urban landscape patterns on air quality trends. Sci. Rep. 10, 1–13. https://doi.org/10.1038/s41598-020-74524-9.
Lim, H., Silvergren, S., Spinicci, S., Mashayekhy Rad, F., Nilsson, U., Westerholm, R., Johansson, C., 2022. Contribution of wood burning to exposures of PAHs and oxy-PAHs in Eastern Sweden. Atmos. Chem. Phys. 22, 11359–11379. https://doi.org/10.5194/acp-22-11359-2022.
Liu, C., Chen, R., Sera, F., Vicedo-Cabrera, A.M., et al., 2019. Ambient particulate air pollution and daily mortality in 652 cities. N. Engl. J. Med. 381, 705–715. https://doi.org/10.1056/nejmoa1817364.
Maenhaut, W., Fernández-Jiménez, M.T., Rajta, I., Artaxo, P., 2002. Two-year study of atmospheric aerosols in Alta Floresta, Brazil: multielemental composition and source apportionment. Nucl. Instruments Methods Phys. Res. Sect. B Beam Interact. Mater. Atoms 189, 243–248. https://doi.org/10.1016/S0168-583X(01)01050-3.
Mallah, Manthar Ali, Changxing, L., Mallah, Mukhtiar Ali, Noreen, S., Liu, Y., Saeed, M., Xi, H., Ahmed, B., Feng, F., Mirjat, A.A., Wang, W., Jabar, A., Naveed, M., Li, J.H., Zhang, Q., 2022. Polycyclic aromatic hydrocarbon and its effects on human health: an overeview. Chemosphere 296. https://doi.org/10.1016/j.chemosphere.2022.133948.
Maselli, B.S., Cunha, V., Lim, H., Bergvall, C., Westerholm, R., Dreij, K., Watanabe, T., Cardoso, A.A., Pozza, S.A., Umbuzeiro, G.A., Kummrow, F., 2020. Similar polycyclic aromatic hydrocarbon and genotoxicity profiles of atmospheric particulate matter from cities on three different continents. Environ. Mol. Mutagen. 61 (560–573) https://doi.org/10.1002/em.22377NIES.
National Institute for Environmental Studies, 2023. Japan. Available at https://www.nies.go.jp/index-e.html. Accessed on 21 September 2023.
NOAA - National Oceanic and Atmospheric Administration, 2023. HYSPLIT Trajectory Mode. Available at: https://ready.arl.noaa.gov/hypub-bin/trajasrc.pl. Accessed 26 Oct. 2023.
Nogueira, T.A.R., Abreu-Junior, C.H., Alleoni, L.R.F., He, Z., Soares, M.R., dos Santos Vieira, C., Lessa, L.G.F., Capra, G.F., 2018. Background concentrations and quality reference values for some potentially toxic elements in soils of São Paulo State. Brazil. J. Environ. Manage. 221, 10–19. https://doi.org/10.1016/j.jenvman.2018.05.048.
Oliveira, César, Martins, N., Tavares, J., Pio, C., Cerqueira, M., Matos, M., Silva, H., Oliveira, Cristina, Camões, F., 2011. Size distribution of polycyclic aromatic hydrocarbons in a roadway tunnel in Lisbon, Portugal. Chemosphere 83, 1588–1596. https://doi.org/10.1016/j.chemosphere.2011.01.011.
Pagliuso, D., Grandis, A., Igarashi, E.S., Lam, E., Buckeridge, M.S., 2018. Correlation of apiose levels and growth rates in duckweeds. Front. Chem. 6, 1–10. https://doi.org/10.3389/fchem.2018.00291.
Pöhlker, C., Wiedemann, K.T., Sinha, B., Shiraiwa, M., Gunthe, S.S., Smith, M., Su, H., Artaxo, P., Chen, Q., Cheng, Y., Elbert, W., Gilles, M.K., Kilcoyne, A.L.D., Moffet, R.C., Weigand, M., Martin, S.T., Pöschl, U., Andreae, M.O., 2012. Biogenic potassium salt particles as seeds for secondary organic aerosol in the Amazon. Science 337, 1075–1079.
Pozza, S.A., Gonçalves, P.B., Wouters, F.C., Vendemiatti, J.A.S., Nogarotto, D.C., Pereira-Filho, E.R., Osório, D.M.M., Romualdo, L.L., Godoi, J.R., Hoinaski, L., Urban, R.C., 2023. Particulate matter pollution and non-targeted analysis of polar compounds in three regions of Brazil. Chemosphere 341. https://doi.org/10.1016/j.chemosphere.2023.139839.
Rahman, M.M., Begum, B.A., Hopke, P.K., Nahar, K., Thurston, G.D., 2020. Assessing the PM2.5 impact of biomass combustion in megacity Dhaka, Bangladesh. Environ. Pollut. 264, 1–11. https://doi.org/10.1016/j.envpol.2020.114798.
Ramdahl, T., 1983. Retene - a molecular marker of wood combustion in ambient air. Nature. https://doi.org/10.1038/306580a0.
Ravishankara, A.R., David, L.M., Pierce, J.R., Venkataraman, C., 2020. Outdoor air pollution in India is not only an urban problem. Proc. Natl. Acad. Sci. USA 117, 28640–28644. https://doi.org/10.1073/pnas.2007236117.
Reff, A., Eberly, S.I., Bhave, P.V., 2007. Receptor modeling of ambient particulate matter data using positive matrix factorization: review of existing methods. J. Air Waste Manage. Assoc. 57, 146–154. https://doi.org/10.1080/10473289.2007.10465319.
Reimann, C., Caritat, P., 2005. Distinguishing between natural and anthropogenic sources for elements in the environment: regional geochemical surveys versus enrichment factors. Sci. Total Environ. 337, 91–107. https://doi.org/10.1016/j.scitotenv.2004.06.011.
Sadiktsis, I., de Oliveira Galvão, M.F., Mustafa, M., Toublanc, M., Ünlü Endirlik, B., Silvergren, S., Johansson, C., Dreij, K., 2023. A yearlong monitoring campaign of polycyclic aromatic compounds and other air pollutants at three sites in Sweden: source identification, in vitro toxicity and human health risk assessment. Chemosphere 332. https://doi.org/10.1016/j.chemosphere.2023.138862.
Santos, A.G., Regis, A.C.D., da Rocha, G.O., de Bezerra, M.A., de Jesus, R.M., de Andrade, J.B., 2016. A simple, comprehensive, and miniaturized solvent extraction method for determination of particulate-phase polycyclic aromatic compounds in air. J. Chromatogr. A 1435, 6–17. https://doi.org/10.1016/j.chroma.2016.01.018.
Scaramboni, C., Urban, R.C., Oliveira, D.P., Dorta, D.J., Campos, M.L.A.M., 2024. Particulate matter from a tropical city in Southeast Brazil: Impact of biomass burning on polycyclic aromatic compounds levels, health risks, and in vitro toxicity. Chemosphere 350, 141072. https://doi.org/10.1016/j.chemosphere.2023.141072.
Schmidl, C., Bauer, H., Dattler, A., Hitzenberger, R., Weissenboeck, G., Marr, I.L., Puxbaum, H., 2008. Chemical characterisation of particle emissions from burning leaves. Atmos. Environ. 42, 9070–9079. https://doi.org/10.1016/j.atmosenv.2008.09.010.
Schraufnagel, D.E., Balmes, J.R., Cowl, C.T., De Matteis, S., Jung, S.H., Mortimer, K., Perez-Padilla, R., Rice, M.B., Riojas-Rodriguez, H., Sood, A., Thurston, G.D., To, T, Vanker, A., Wuebbles, D.J., 2019. Air Pollution and noncommunicable diseases: a review by the forum of international respiratory societies' environmental committee, part 1: the damaging effects of air pollution. Chest 155, 409–416. https://doi.org/10.1016/j.chest.2018.10.042.
SGU - Sveriges geologiska Undersökning, 2007. Geokemiska Kartan Markgeokemi. Metaller i Morän Och Andra Sediment Östra Mälardalen med Stockholm, Uppsala.
Silva, R.M., Lopes, A.G., Santos, C.A.G., 2023. Deforestation and fires in the Brazilian Amazon from 2001 to 2020 : impacts on rainfall variability and land surface temperature. J. Environ. Manag. 326, 116664 https://doi.org/10.1016/j.jenvman.2022.116664.
Simoneit, B.R.T., 2002. Biomass Burning — A Review of Organic Tracers for Smoke from Incomplete Combustion.
SLB, 2021. Luften i Stockholm. Årsrapport 2021.
Suciu, L.G., Masiello, C.A., Griffin, R.J., 2019. Anhydrosugars as Tracers in the Earth System, Biogeochemistry. Springer International Publishing. https://doi.org/10.1007/s10533-019-00622-0.

Taner, S., Pekey, B., Pekey, H., 2013. Fine particulate matter in the indoor air of barbeque restaurants: elemental compositions, sources and health risks. Sci. Total Environ. 454–455, 79–87. https://doi.org/10.1016/j.scitotenv.2013.03.018.

Tobiszewski, M., Namieśnik, J., 2012. PAH diagnostic ratios for the identification of pollution emission sources. Environ. Pollut. 162, 110–119. https://doi.org/10.1016/j.envpol.2011.10.025.

Urban, R.C., Lima-Souza, M., Caetano-Silva, L., Queiroz, M.E.C., Nogueira, R.F.P., Allen, A.G., Cardoso, A.A., Held, G., Campos, M.L.A.M., 2012. Use of levoglucosan, potassium, and water-soluble organic carbon to characterize the origins of biomass-burning aerosols. Atmos. Environ. 61, 562–569. https://doi.org/10.1016/j.atmosenv.2012.07.082.

Urban, R.C., Alves, C.A., Allen, A.G., Cardoso, A.A., Queiroz, M.E.C., Campos, M.L.A.M., 2014. Sugar markers in aerosol particles from an agro-industrial region in Brazil. Atmos. Environ. 90, 106–112. https://doi.org/10.1016/j.atmosenv.2014.03.034.

Varmuza, K., Filzmoser, P., 2009. Principal Component Analysis. In: Introduction to Multivariate Statistical Analysis in Chemometrics, Boca Raton. CRC Press, pp. 73–117.

Vithanage, M., Bandara, P.C., Novo, L.A.B., Kumar, A., Ambade, B., Naveendrakumar, G., Ranagalage, M., Magana-Arachchi, D.N., 2022. Deposition of trace metals associated with atmospheric particulate matter: Environmental fate and health risk assessment. Chemosphere 303, 135051. https://doi.org/10.1016/j.chemosphere.2022.135051.

Wang, X., Sato, T., Xing, B., 2006. Size distribution and anthropogenic sources apportionment of airborne trace metals in Kanazawa, Japan. Chemosphere 65, 2440–2448. https://doi.org/10.1016/j.chemosphere.2006.04.050.

WHO - World Health Organization, 2000. Air Quality Guidelines for Europe, Second edition, Copenhagen.

WHO - World Health Organization, 2021. WHO Global Air Quality Guidelines. Particulate Matter (PM2.5 and PM10), Ozone, Nitrogen Dioxide, Sulfur Dioxide and Carbon Monoxide, Geneva.

WHO Europe, 2021. Human Health Effects of Polycyclic Aromatic Hydrocarbons as Ambient Air Pollutants: Report of the Working Group on Polycyclic Aromatic Hydrocarbons of the Joint Task Force on the Health Aspects of Air Pollution, Copenhagen.

Wolf, K., Hoffmann, B., Andersen, Z.J., Atkinson, R.W., et al., 2021. Long-term exposure to low-level ambient air pollution and incidence of stroke and coronary heart disease: a pooled analysis of six European cohorts within the ELAPSE project. Lancet Planet. Heal. 5, e620–e632. https://doi.org/10.1016/S2542-5196(21)00195-9.

Wu, Y., Salamova, A., Venier, M., 2021. Using diagnostic ratios to characterize sources of polycyclic aromatic hydrocarbons in the Great Lakes atmosphere. Sci. Total Environ. 761, 143240 https://doi.org/10.1016/J.SCITOTENV.2020.143240.

Yamasaki, S., Takeda, A., Nunohara, K., Tsuchiya, N., 2013. Red soils derived from limestone contain higher amounts of trace elements than those derived from various other parent materials. Soil Sci. Plant Nutr. 59, 692–699. https://doi.org/10.1080/00380768.2013.822301.

Yamashina Website, 2023. Populatioin and Number of Households [WWW Document]. URL. https://www.city.kyoto.lg.jp/yamasina/. accessed 10.26.23.

Yan, B., Abrajano, T.A., Bopp, R.F., Chaky, D.A., Benedict, L.A., Chillrud, S.N., 2005. Molecular tracers of saturated and polycyclic aromatic hydrocarbon inputs into Central Park Lake, New York City. Environ. Sci. Technol. 39, 7012–7019. https://doi.org/10.1021/es0506105.

Ye, T., Xu, R., Yue, X., Chen, G., Yu, P., Coêlho, M.S.Z.S., Saldiva, P.H.N., Abramson, M. J., Guo, Y., Li, S., 2022. Short-term exposure to wildfire-related PM2.5 increases mortality risks and burdens in Brazil. Nat. Commun. 13, 1–9. https://doi.org/10.1038/s41467-022-35326-x.

Yu, P., Xu, R., Li, S., Yue, X., Chen, G., Ye, T., Coêlho, M.S.Z.S., Saldiva, P.H.N., Sim, M. R., Abramson, M.J., Guo, Y., 2022. Exposure to wildfire-related PM2.5 and site-specific cancer mortality in Brazil from 2010 to 2016: a retrospective study. PLoS Med. 19, e1004103 https://doi.org/10.1371/journal.pmed.1004103.

Yunker, M.B., Macdonald, R.W., Vingarzan, R., Mitchell, R.H., Goyette, D., Sylvestre, S., 2002. PAHs in the Fraser River basin: a critical appraisal of PAH ratios as indicators of PAH source and composition. Org. Geochem. 33, 489–515. https://doi.org/10.1016/S0146-6380(02)00002-5.

Zhang, Z., Gao, J., Engling, G., Tao, J., Chai, F., Zhang, L., Zhang, R., Sang, X., Chan, C. Y., Lin, Z., Cao, J., 2015. Characteristics and applications of size-segregated biomass burning tracers in China's Pearl River Delta region. Atmos. Environ. 102, 290–301. https://doi.org/10.1016/j.atmosenv.2014.12.009.